NAVORD REPORT 3759

SELF-COMPENSATED MULTILAYER DISTRIBUTED CONSTANT DELAY LINES

7 OCTOBER 1954

U. S. NAVAL ORDNANCE LABORATORY
WHITE OAK, MARYLAND

NAVORD Report 3759

SELF COMPENSATED MULTILAYER DISTRIBUTED CONSTANT DELAY LINES

Prepared by:

William S. Carley

ABSTRACT: The inductance of a line is known to decrease with frequency. The stray capacitance between turns is actually in parallel with the inductance of a turn. This forms a parallel circuit which can help offset the variation of inductance with frequency. In the multilayer case the stray capacitance is increased many times. From these principles, design equations are developed for the multilayer line.

In the impedance range of 2,500 to 10,000 ohms these lines have delays ranging from 0.05 to 0.5 microsecond per axial inch. These lines have characteristic impedances which are at least three times greater than conventional lines and delay times per unit length of about 10 times that of delay line cable.

Experimental results in the form of photographs of the pulse response of several of these lines to pulse durations of 1.0 microsecond are given. RG-65 U delay line cable is used for comparison.

Experimental results show that the rise time of multilayer lines can be shorter than commercial delay line cable if the delay is in the vicinity of 4 microseconds.

The investigation was made as part of Foundational Research Task Numbers FR-4-52, FR-4-53, and FR-29-54.

U. S. NAVAL ORDNANCE LABORATORY
WHITE OAK, MARYLAND

The results of an investigation of high impedance delay lines are given in this report. References are made in the text to the following publications:

References

1. Wm. S. Carley and Edward F. Seymour "High Characteristic Impedance Distributed Constant Delay Lines for Fractional Microsecond Pulses", Proc. N.E.C., vol 8, pp 787-789; 1953
2. Wm. S. Carley and Edward F. Seymour "High Impedance Artificial Delay Lines", Electronics, vol 26, pp 188-194; Apr 1953
3. Wm. S. Carley "Distributed Constant Delay Lines with Characteristic Impedances Higher Than 5000 Ohms", Convention Record of the I.R.E. Part 5, pp 71-80; 1953
4. Wm. S. Carley "Self-Compensated Multilayer Distributed Constant Delay Lines", Proc. N.E.C., vol 9, pp 150-160; 1954
5. Wm. S. Carley "Multilayer Distributed Constant Delay Lines", Tele-Tech & Electronic Industries, May 1954, p 74
6. Blewitt, Langmuir, Nelson and Rubel "Delay Lines", General Electric Rpt. May 31, 1943. Similar to T. P. Blewett and J. H. Rubel "Video Delay Lines", Proc. I.R.E., vol 35 pp 1580-1584; 1947
7. G. N. Watson "Theory of Bessel Functions", Cambridge University Press, Cambridge, England; 1922
8. Stanford Goldman "Frequency Analysis Modulation and Noise", McGraw-Hill Book Co., New York, New York, p 120; 1948
9. R. A. Erickson and H. Sommer "The Compensation of Delay Distortion in Video Delay Lines", Proc. I.R.E., vol 38, pp 1036-1040; 1950
10. Ernst Weber "Electromagnetic Fields, Theory and Application", vol 1, John Wiley and Sons, New York, New York, p 150; 1953
11. David K. Cheng, "A Note on the Reproduction of Pulses", Proc. I.R.E., vol 40, p 963; 1952

JOHN T. HAYWARD
Captain, USN
Commander

H. J. PLUMLEY
By direction

CONTENTS

ILLUSTRATIONS

SELF COMPENSATED MULTILAYER DISTRIBUTED CONSTANT DELAY LINES

INTRODUCTION

1. Increasing application is being made of distributed constant delay lines as circuit elements in present day electronic equipment. The characteristic impedance of these lines has been limited to values between 400 and 3,000 ohms and delay times up to 1/2 microsecond per foot. The author recently reported preliminary investigations on multilayer bank wound delay lines with impedances from 5,000 to 10,000 ohms and delay times up to 1/2 microsecond per inch[1,2,3,4,5]. The object of this report is to consolidate the theoretical work in the design of multilayer lines with experimental results in the impedance range of 2,500 to 10,000 ohms.

Theory

2. Figure 1 is a view of the line, with a section taken along the axis of the solenoid. The line is assumed to be infinite in length and of a multilayer bank wound construction with capacitance to ground. In general the line was wound over the ground as shown in Figure 1 but several lines were wound with the ground over the line. Z is taken along the axial direction of the winding. It is assumed that a mutual inductance exists between two elementary lengths of the wire which is dependent solely on the distance between them. A stray capacitance also exists between each turn and several of its neighbors. The overall diameter of the wire with its insulation is b and that of the uninsulated wire is a. The number of layers in the bank winding is p. It is assumed that the wire in traveling from a top layer to a bottom layer, does not take up any space. It is further assumed that the diameter D is a small part of a wave length at the highest frequency of interest.

3. The schematic diagram of the line in terms of lumped parameters is shown in Figure 2. The section of the uniform line dZ in length is characterized by a shunt conductance $dG = GdZ$, a shunt capacitance $dC = C_0dZ$, and a series resistance $dR = RdZ$. The structure is further complicated by the stray capacitance between turns and by the fact that the total phase shift is so large that the inductance of the infinitesimal section under study is influenced by the phase of the current flowing in many other turns. It is assumed that the phase difference between the currents in the other turns is dependent on the distance between them and the turn under consideration.

4. It will be assumed that the characteristics of the line can be deduced from the characteristics of any one elementary section taking into account the effects of other sections on the elementary section.

5. As in standard transmission line procedure we will assume a definite input current and voltage, and calculate the output current and voltage from the constants of the line. As the line sections are already reduced to infinitesimal sections we may neglect the shunt elements in the computation of the effect of the series elements and vice versa.

6. In each section of the line the voltage is decreased because of the series impedance and the current decreased by the action of the shunt admittance and the stray capacitance. In order to simplify the derivation it will now be assumed that the current and voltage are sinusoidally distributed in the axial direction (Z) except in the calculation of the effective series inductance and the effects of the stray capacitance. This is a very good approximation as the lines have a very low loss and in fact will later be assumed lossless to further simplify the resulting equations.

7. Noting that a dot over the quantity is used to denote a vector the equations of the voltage drop across an infinitesimal section of line and the shunt current may be written as

$$-dv(\dot{w}'',t) = Ri(\dot{w}'',t)d\dot{w}''+\left[\int_{w'=-\infty}^{\infty} m(\dot{w})\frac{\partial}{\partial t} i(\dot{w}',t)d\dot{w}'\right] d\dot{w}'' \qquad (1)$$

and

$$-di(\dot{w}'',t) = Gv(\dot{w}'',t)d\dot{w}''+C_0\frac{\partial}{\partial t} v(\dot{w}'',t)d\dot{w}''+\left[\int_{w'=-\infty}^{\infty} c(\dot{w})\frac{\partial}{\partial t}\left[v(\dot{w}'',t) -v(\dot{w}',t)\right] d\dot{w}'\right] d\dot{w}''. \qquad (2)$$

where v = alternating component of the voltage,
i = alternating component of the current,
R = resistance per unit length (mhos/meter),
G = conductance per unit length (mhos/meter),
C_0 = capacitance to core per unit length (farads/meter),
$m(w)$ = mutual inductance per unit length between two elementary sections of line length dZ and dZ' separated by a distance $\dot{w}$ (henries/meter),

$\dot{w} = (\dot{z}'-\dot{z}+\dot{r}'-\dot{r}) = \dot{w}' - \dot{w}''$
$\dot{w}' = \dot{z}'+\dot{r}'$
$\dot{w}'' = \dot{z}+\dot{r}$

let $i = I_{max} \exp j\omega(t-\frac{\dot{w}'}{V})$

and $v = V_{max} \exp j\omega(t-\frac{\dot{w}'}{V})$

where $\omega = \frac{2\pi V}{\lambda} = 2\pi f$

V = velocity of propagation.

Let us look at $\int_{-\infty}^{\infty} m(\dot{w}) \frac{\partial}{\partial t} i(\dot{w}', t) d\dot{w}'$,

$$= j\omega I \int_{-\infty}^{\infty} m(\dot{w}) \exp j\omega\left(t - \frac{\dot{w}'}{v}\right) d\dot{w}',$$

$$= j\omega I \exp j\omega\left(t - \frac{\dot{w}''}{v}\right) \int_{-\infty}^{\infty} m(\dot{w}) \exp\left(-j\frac{\omega \dot{w}}{v}\right) d\dot{w},$$

$$= j\omega i \, L\left(\frac{\omega}{v}\right), \qquad (4)$$

where $L\left(\frac{\omega}{v}\right) = \int_{-\infty}^{\infty} m(\dot{w}) \exp\left(-j\frac{\omega \dot{w}}{v}\right) d\dot{w}, \qquad (5)$

thus $L\left(\frac{\omega}{v}\right)$ is the Fourier transform of $m(\dot{w})$

8. This problem may be simplified considerably by the following approximation. Let us assume that the radial depth of the winding pb $\ll \frac{D}{2}$ and in fact is so small that $(r'-r) \longrightarrow 0$. In other words we assume we have a single layer solenoid wound with wire whose diameter is $\frac{b}{p}$. This assumption has been experimentally verified as will be shown later. In practice $\frac{D}{2}$ would have a lower limit of about 0.07" and pb upper limit about 0.012" so that r' would vary from 0.064" to 0.076".

9. The parameter w then becomes a function of the axial separation between the reference turn and all other turns. This problem has been solved[6]. The authors replaced the coil with a thin cylindrical sheet of radius $\frac{D}{2}$ over which flows a current sheet in the axial direction

$$I_s = I_o \exp(-\beta Z) \qquad \text{per unit length}$$

where $\beta = \frac{2\pi}{\lambda}$

The solution of equation (5) was given as

$$L\left(\frac{\omega}{v}\right) = \left[2I_1\left(\frac{\pi D}{\lambda}\right) K_1\left(\frac{\pi D}{\lambda}\right)\right] L_o, \qquad (6)$$

where I_1 and K_1 are modified Bessel Functions of the first and second kind[7],

L_o = inductance of the line at low frequencies (henries/meter),
D = mean line diameter (meters),
λ = axial wave length along the line (meters).

10. We now determine the capacitance coupling to the n th coil by considering the effect of the nearest neighboring coils only. Inasmuch as the variable of integration in equation (2) is $\dot{w}'$

one can take the differentiation sign out of the integral thus

$$\int_{-\infty}^{\infty} c(\dot{w}) \frac{\partial}{\partial t} \left[v(\dot{w}'', t) - v(\dot{w}', t) \right] d\dot{w}' = \frac{\partial}{\partial t} \int_{-\infty}^{\infty} c(\dot{w}) \left[v(\dot{w}'', t) - v(\dot{w}', t) \right] d\dot{w}' . \tag{7}$$

11. As the capacitance per unit length is constant equation (7) becomes

$$= \frac{C_t}{b} \frac{\partial}{\partial t} \int_{-\infty}^{\infty} \left[v(\dot{w}'', t) - v(\dot{w}', t) \right] d\dot{w}', \tag{8}$$

Where C_t = stray capacitance between two adjacent turns and $\frac{C_t}{b}$ = stray capacitance/unit length.

$$\int_{-\infty}^{\infty}\left[v(w'',t) - v(w',t)\right] d w' = -\left[(v_{n-p-1} - v_n) + (v_{n-p} - v_n) + (v_{n-1} - v_n) - (v_n - v_{n+1}) - (v_n - v_{n+p}) - (v_n - v_{n+p+1})\right] \quad (9)$$

If the n th turn had been on the inside boundary

$$\int_{-\infty}^{\infty}\left[v(\dot{w}'',t) - v(\dot{w}',t)\right] dw' = -\left[(v_{n-p} - v_n) - (v_n - v_{n+1}) - (v_n - v_{n+p}) - (v_n - v_{n+p+1})\right]. \quad (10)$$

If the n th turn had been on the outside boundary

$$\int_{-\infty}^{\infty}\left[v(\dot{w}'',t) - v(\dot{w}',t)\right] dw' = -\left[(v_{n-p-1} - v_n) + (v_{n-p} - v_n) + (v_{n-1} - v_n) - (v_n - v_{n+p})\right]. \quad (11)$$

Expanding by means of a Taylor series for the voltage of the adjacent turn in reference to that of its neighboring turn and substituting x for w'

$$v_{n+1} = v_n + b\,\frac{dv_n}{dx} + \frac{b^2}{2!}\,\frac{d^2v_n}{dx^2} + \ldots\ldots \quad (12)$$

$$v_{n-1} = v_n - b\,\frac{dv_n}{dx} + \frac{b^2}{2!}\,\frac{d^2v_n}{dx^2} - \ldots\ldots \quad (13)$$

$$v_{n+p} = v_{n+p-1} + b\,\frac{d(v_{n+p-1})}{dx} + \frac{b^2}{2!}\,\frac{d^2(v_{n+p-1})}{dx^2} + \ldots \quad (14)$$

$$v_{n-p} = v_{n-p+1} - b\,\frac{(dv_{n-p+1})}{dx} + \frac{b^2}{2!}\,\frac{d^2(v_{n-p+1})}{dx^2} - \ldots \quad (15)$$

$$v_{n+p-1} = v_{n+p-2} + b\,\frac{d(v_{n+p-2})}{dx} + \frac{b^2}{2!}\,\frac{d^2(v_{n+p-2})}{dx^2} + \ldots \quad (16)$$

$$v_{n+p-2} = v_{n+p-3} + b\,\frac{d(v_{n+p-3})}{dx} + \frac{b^2}{2!}\,\frac{d^2(v_{n+p-3})}{dx^2} + \ldots \quad (17)$$

$$v_{n+p+1} = v_{n+p} + b\,\frac{d(v_{n+p})}{dx} + \frac{b^2}{2!}\,\frac{d^2}{dx^2}(v_{n+p}) + \frac{b^3}{3!}\,\frac{d^3}{dx^3}(v_{n+p}) \quad (18)$$

Substituting equation (14) in equation (18) we obtain

$$v_{n+p+1} = v_{n+p-1} + b\frac{d}{dx}(v_{n+p-1}) + \frac{b^2}{2!}\frac{d^2}{dx^2}(v_{n+p-1}) + \frac{b^3}{3!}\frac{d^3}{dx^3}(v_{n+p-1})$$

$$+ b\left[\frac{d}{dx}(v_{n+p-1}) + b\frac{d^2}{dx^2}(v_{n+p-1}) + \frac{b^2}{2!}\frac{d^3}{dx^3}(v_{n+p-1}) + \cdots\right]$$

$$+ \frac{b^2}{2!}\left[\frac{d^2}{dx^2}(v_{n+p-1}) + b\frac{d^3}{dx^3}(v_{n+p-1}) + \frac{b^2}{2}\frac{d^4}{dx^4}(v_{n+p-1}) + \cdots\right]$$

$$+ \frac{b^3}{3!}\left[\frac{d^3}{dx^3}(v_{n+p-1}) + b\frac{d^4}{dx^4}(v_{n+p-1})\right] + \cdots \quad (19)$$

Collecting terms

$$v_{n+p+1} = v_{n+p-1} + 2b\frac{d}{dx}(v_{n+p-1}) + 2b^2\frac{d^2}{dx^2}(v_{n+p-1}) + \frac{4b^3}{3}\frac{d^3}{dx^3}(v_{n+p-1})$$

$$+ \frac{2b^4}{3}\frac{d^4}{dx^4}(v_{n+p-1}) + \cdots \quad (20)$$

Substituting equation (14) in equation (18)

$$v_{n+p+1} = v_{n+p-2} + b\frac{d}{dx}(v_{n+p-2}) + \frac{d^2}{2!}\frac{d}{dx}(v_{n+p-2}) + \cdots$$

$$+ 2b\left[\frac{d}{dx}(v_{n+p-2}) + b\frac{d^2}{dx^2}(v_{n+p-2}) + \cdots\right] + 2b^2\left[\frac{d^2}{dx^2}(v_{n+p-2}) + \cdots\right]$$

$$+ \frac{4b^3}{3}\left[\frac{d^3}{dx^3}(v_{n+p-2}) + \cdots\right] + \frac{2b^4}{3}\left[\frac{d^4}{dx^4}(v_{n+p-2}) + \cdots\right] + \cdots \quad (21)$$

Collecting terms

$$v_{n+p+1} = v_{n+p-2} + 3b\frac{d}{dx}(v_{n+p-2}) + \frac{5b^2}{2}\frac{d^2}{dx^2}(v_{n+p-2}) + \frac{9b^3}{2}\frac{d^3}{dx^3}(v_{n+p-2})$$

$$+ \frac{81b^4}{24}\frac{d^4}{dx^4}(v_{n+p-2}) + \cdots \quad (22)$$

Substituting equation (17) in equation (22)

$$v_{n+p+1} = v_{n+p-3} + 4b\frac{d}{dx}(v_{n+p-3}) + 6b^2\frac{d^2}{dx^2}(v_{n+p-3}) + \frac{26b^3}{3}\frac{d^3}{dx^3}(v_{n+p-3})$$

$$\frac{29b^4}{3}\frac{d^4}{dx^4}(v_{n+p-2}) + \cdots \quad (23)$$

In similar fashion

$$v_{n+p+1} = v_{n+p-4} + 5b \frac{d}{dx}(v_{n+p-4}) + \frac{21b^2}{2} \frac{d^2}{dx^2}(v_{n+p-4})$$

$$+ \frac{101b^3}{6} \frac{d^3}{dx^3}(v_{n+p-4}) + \frac{529b^4}{24} \frac{d^4}{dx^4}(v_{n+p-4}) + \cdots \quad (24$$

$$v_{n+p+1} = v_{n+p-5} + 6b \frac{d}{dx}(v_{n+p-5}) + 16b^2 \frac{d^2}{dx^2}(v_{n+p-5})$$

$$\frac{180b^3}{6} \frac{d^3}{dx^3}(v_{n+p-5}) + \frac{1080b^4}{24} \frac{d^4}{dx^4}(v_{n+p-4}) + \quad (25)$$

Thus

$$v_{n+p+1} = v_{n+p-6} + 7b \frac{d}{dx}(v_{n+p-6}) + \frac{45b^2}{2} \frac{d^2}{dx^2}(v_{n+p-6})$$

$$+ \frac{295b^3}{6} \frac{d^3}{dx^3}(v_{n+p-6}) + \frac{2017b^4}{24} \frac{d^4}{dx^4}(v_{n+p-4}) + \cdots \quad (26)$$

etc until we get a series for v_{n+p+1} in terms of v_n

similarly

$$v_{n-p-1} = v_{n-p} - b \frac{d}{dx}(v_{n-p}) + \frac{b^2}{2} \frac{d^2}{dx^2}(v_{n-p}) - \frac{b^3}{3} \frac{d^3}{dx^3}(v_{n-p})$$

$$\frac{b^4}{4} \frac{d^4}{dx^4}(v_{n-p}) \quad (27)$$

$$= v_{n-p+1} - b \frac{d}{dx}(v_{n-p+1}) + \frac{b^2}{2} \frac{d^2}{dx^2}(v_{n-p+1}) - \cdots$$

$$- b\left[\frac{d}{dx}(v_{n-p+1}) - b \frac{d^2}{dx^2}(v_{n-p+1}) + \frac{b^2}{2} \frac{d^3}{dx^3}(v_{n-p+1}) - \cdots\right]$$

$$+ \frac{b^2}{2}\left[\frac{d^2}{dx^2}(v_{n-p+1}) - b \frac{d^3}{dx^3}(v_{n-p+1}) + \frac{b^2}{2} \frac{d^4}{dx^4}(v_{n-p+1}) - \cdots\right]$$

$$- \frac{b^3}{3}\left[\frac{d^3}{dx^3}(v_{n-p+1}) - b \frac{d^4}{dx^4}(v_{n-p+1}) + \cdots\right] + \frac{b^4}{4}\left[\frac{d^4}{dx^4}(v_{n-p+1}) - \cdots\right] \quad (28$$

$$= v_{n-p+1} - 2b \frac{d}{dx}(v_{n-p+1}) + \frac{2b^2}{} \frac{d^2}{dx^2}(v_{n-p+1}) - \frac{5b^3}{3} \frac{d^3}{dx^3}(v_{n-p+1})$$

$$+ \frac{17b^4}{12} \frac{d^4}{dx^4}(v_{n-p+1}) - \cdots \quad (29)$$

$$= v_{n-p+2} - 3b \frac{d}{dx}(v_{n-p+2}) + \frac{5b^2}{2} \frac{d^2}{dx^2}(v_{n-p+2}) - \frac{5b^3}{} \frac{d^3}{dx^3}(v_{n-p+2})$$

$$+ \frac{5b^4}{} \frac{d^4}{dx^4}(v_{n-p+2}) - \cdots \quad (30)$$

$$= v_{n-p+3} - 4b \frac{d}{dx}(v_{n-p+3}) + 6b^2 \frac{d^2}{dx^2}(v_{n-p+3}) - \frac{28b^3}{3} \frac{d^3}{dx^3}(v_{n-p+3})$$

$$+ \frac{25b^4}{2} \frac{d^4}{dx^4}(v_{n-p+3}) - \cdots \quad (31)$$

$$= v_{n-p+4} - 5b \frac{d}{dx}(v_{n-p+4}) + \frac{21b^2}{2} \frac{d^2}{dx^2}(v_{n-p+4}) - \frac{53b^3}{3} \frac{d^3}{dx^3}(v_{n-p+4})$$

$$+ \frac{317b^4}{12} \frac{d^4}{dx^4}(v_{n-p+4}) - \cdots \quad (32)$$

etc until we get a series for v_{n-p-1} in terms of v_n

If q is the number of turns removed from the reference turn a general expression would be

$$v_{n\pm q} = v_n \pm qb \frac{d}{dx}(v_n) + b^2 \left[\frac{q^2}{2} - A\right] \frac{d^2}{dx^2}(v_n)$$

$$\pm b^3 \left[\frac{q^3}{3!} - B\right] \frac{d^3}{dx^3}(v_n) + b^4 \left[\frac{q^4}{4!} - C\right] \frac{d^4}{dx^4}(v_n)$$

$$\pm b^5 \left[\frac{q^5}{5!} - D\right] \frac{d^5}{dx^5}(v_n), \quad (33)$$

where

$$A \begin{cases} = 0 & q < 3 \\ = \dfrac{2\,(q-3)^0}{0!} = 2 & q \geq 3 \end{cases}$$

$$B \begin{cases} = 0 & q < 4 \\ = \dfrac{2\,(q-3)}{1!} & q \geq 4 \end{cases}$$

$$C \begin{cases} = 0 & q < 4 \\ = \dfrac{2\,(q-3)^2}{2!} & q \geq 4 \end{cases}$$

$$D \begin{cases} = 0 & q < 4 \\ = 2\,\dfrac{(q-3)^3}{3!} & q \geq 4 \end{cases}$$

For an inside turn using equations (9) and (33)

$$\int_{-\infty}^{\infty} \left[v(w'',t) - v(w',t) \right] dw' = -\Big\{ b(p+1)\,\frac{d}{dx}\,v_n + \frac{b^2}{2!}\left[(p+1)^2 - A' \right] \frac{d^2}{dx^2}\,v_n$$

$$- \frac{b^3}{3!}\left[(p+1)^3 - B' \right] \frac{d^3}{dx^3}\,v_n + \frac{b^4}{4!}\left[(p+1)^4 - C' \right] \frac{d^4}{dx^4}\,v_n - \cdots$$

$$- nb\,\frac{d}{dx}\,v_n + \frac{b^2}{2!}\left[p^2 - A'' \right] \frac{d^2}{dx^2}\,v_n - \frac{b^3}{3!}\left[p^3 - B'' \right] \frac{d^3}{dx^3}\,v_n$$

$$\frac{b^4}{4!}\left[p^4 - C'' \right] \frac{d^4}{dx^4}\,v_n - \cdots - b\,\frac{d}{dx}\,v_n + \frac{b^2}{2!}\,\frac{d^2}{dx^2}\,v_n$$

$$- \frac{b^3}{3!}\,\frac{d^3}{dx^3}\,v_n + \frac{b^4}{4!}\,\frac{d^4}{dx^4}\,v_n - \cdots + b\,\frac{d}{dx}\,v_n + \frac{b^2}{2!}\,\frac{d^2}{dx^2}\,v_n$$

$$+ \frac{b^3}{3!}\,\frac{d^3}{dx^3}\,v_n + \frac{b^4}{4!}\,\frac{d^4}{dx^4}\,v_n - \cdots + pb\,\frac{d}{dx}\,v_n$$

$$+ \frac{b^2}{2!}\left[p^2 - A'' \right] \frac{d^2}{dx^2}\,v_n + \frac{b^3}{3!}\left[p^3 - B'' \right] \frac{d^3}{dx^3}\,v_n + \frac{b^4}{4!}\left[p^4 - C'' \right] \frac{d^4}{dx^4}\,v_n + \cdots$$

$$+ b(p+1)\,\frac{d}{dx}\,v_n + \frac{b^2}{2!}\left[(p+1)^2 - A''' \right] \frac{d^2}{dx^2}\,v_n + \frac{b^3}{3!}\left[(p+1)^3 - B''' \right] \frac{d^3}{dx^3}\,v_n$$

$$+ \frac{b^4}{4!}\left[(p+1)^4 - C''' \right] \frac{d^4}{dx^4}\,v_n \Big\} \qquad (34)$$

$$\int_{-\infty}^{\infty} \left[v(w'',t) - v(w',t) \right] dw' = -\Big\{ \frac{b^2}{2!}\left[4p^2 + 4p + 4 - A^* \right] \frac{d^2}{dx^2}\,v_n$$

$$- C^*\,\frac{d^3}{dx^3}\,v_n + \frac{b^4}{4!}\left[4p^3 + 8p^3 + 12p^2 + 8p + 4 - C^* \right] \frac{d^4}{dx^4}\,v_n \Big\} \qquad (35)$$

where $A^* \begin{cases} 0 & p < 2 \\ 4 \text{ if } & p = 2 \\ 8 & p \geq 3 \end{cases}$

C^* will not be needed later and is not tabulated

From an inside boundary turn using equations (10) and (33)

$$\int_{-\infty}^{w''} \left[v(w'',t) - v(w',t) \right] dw' = \left\{ -pb \frac{d}{dx} v_n + b^2 \left[\frac{p^2}{2!} - A'' \right] \frac{d^2}{dx^2} v_n \right.$$

$$- \frac{b^3}{} \left[\frac{p^3}{3!} - B'' \right] \frac{d^3}{dx^3} v_n + b^4 \left[\frac{p^4}{4!} - C'' \right] \frac{d^4}{dx^4} v_n + \frac{b}{} \frac{d}{dx} v_n$$

$$+ \frac{b^2}{2!} \frac{d^2}{dx^2} v_n + \frac{b^3}{3!} \frac{d^3}{dx^3} v_n + \frac{b^4}{4!} \frac{d^4}{dx^4} v_n$$

$$pb \frac{d}{dx} v_n + b^2 \left[\frac{p^2}{2!} - A'' \right] \frac{d^2}{dx^2} v_n + b^3 \left[\frac{p^3}{3!} - B'' \right] \frac{d^3}{dx^3} v_n + b^4 \left[\frac{p^4}{4!} - C'' \right] \frac{d^4}{dx^4} v_n +$$

$$+ b(p+1) \frac{d}{dx} v_n + b^2 \left[\frac{(p+1)^2}{2!} - A''' \right] \frac{d^2}{dx^2} v_n + b^3 \left[\frac{(p+1)^3}{3!} - B''' \right] \frac{d^3}{dx^3} v_n$$

$$\left. + b^4 \left[\frac{(p+1)^4}{4!} - C''' \right] \frac{d^4}{dx^4} v_n \right\} \qquad (36)$$

$$\int_{-\infty}^{w''} \left[v(w'',t) - v(w',t) \right] dw' = \left\{ (p+2) \frac{bd}{dx} v_n + b^2 \left[\frac{3p^2 + 2p + 2}{2!} - A^* \right] \frac{d^2}{dx^2} v_n \right.$$

$$\left. + b^3 \left[\frac{p^3 + 3p^2 + 3p + 2}{3!} - B^* \right] \frac{d^3}{dx^3} v_n + b^4 \left[3 \frac{p^4 + 4p^3 + 6p^2 + 4p + 2}{4!} - C^* \right] \frac{d^4}{dx^4} v_n \right\}$$

where $$A^* = \begin{cases} 0 & p < 2 \\ 2 & \text{if } p = 2 \\ 6 & p \geq 3 \end{cases}$$

for an outside boundary turn using equations (11) and (33)

$$\int_{w''}^{\infty} \left[v(w''t) - v(w',t) \right] dw' = \left\{ -(p+1) \frac{bd}{dx} v_n \right.$$

$$+ b^2 \left[\frac{(p+1)^2}{2!} - A' \right] \frac{d^2}{dx^2} v_n - b^3 \left[\frac{(p+1)^3}{3!} - B' \right] \frac{d^3}{dx^3} v_n$$

$$+ \frac{b^4}{} \left[\frac{(p+1)^4}{4!} - C' \right] \frac{d^4}{dx^4} v_n + \ldots - p \frac{bd}{dx} v_n + b^2 \left[\frac{p^2}{2!} - A'' \right] \frac{d^2}{dx^2} v_n$$

$$- b^3\left[\frac{p^3}{3!} - B''\right]\frac{d^3}{dx^3} v_n + b^4\left[\frac{p^4}{4!} - C''\right]\frac{d^4}{dx^4} v_n - \cdots$$

$$- \frac{b}{} \frac{d}{dx} v_n + \frac{b^2}{2!} \frac{d^2}{dx^2} v_n - \frac{1b^3}{3!} \frac{d^3}{dx^3} v_n + \frac{b^4}{4!} \frac{d^4}{dx^4} v_n - \cdots$$

$$+ \frac{pb}{} \frac{d}{dx} v_n + b^2\left[\frac{p^2}{2!} - A''\right]\frac{d^2}{dx^2} v_n + b^3\left[\frac{p^3}{3!} - B''\right]\frac{d3}{dx^3} v_n$$

$$\frac{b^4}{}\left[\frac{p^4}{4!} - C''\right]\frac{d^4}{dx^4} v_n + \cdots \Bigg\} \tag{38}$$

$$\int_{-\infty}^{\infty}\left[v(\dot{w}''t) - v(w',t)\right] dw' = -\Bigg\{-(p+2)\ b\frac{d}{dx} v_n + b^2\left[\frac{3p^2+2p+2}{2} - A^{o*}\right]\frac{d^2}{dx^2} v_n$$

$$- b^3\left[\frac{p^3-3p^2}{3!} \frac{3p}{} - B^{o*}\right]\frac{d^3}{dx^3} v_n + b^4\left[3\ \frac{p^4-4p^3+6p^2-4p+2}{4!} - C^{o*}\right]\frac{d^4}{dx^4} v_n\Bigg\}$$

where $A^{o*} = \begin{cases} o & p < 2 \\ 2 & p = 2 \\ 6 & p \geq 3 \end{cases}$ (39)

To a first approximation we may neglect all terms higher than the second derivative if the phase shift per turn is small.

$$\int_{-\infty}^{\infty} v(\dot{w}'',t) - v(\dot{w}'t)\ d\dot{w}' = -b^2\left[\frac{(p^2+p+1)2}{} - A^*\right]\frac{d^2}{dx^2} v_n \text{ for an inside turn} \tag{40}$$

$$= -b(p+2)\ \frac{d}{dx} v_n - \frac{b^2}{}\left[\frac{3p^2+2p+2}{2!} - A^*\right]\frac{d^2}{dx^2} v_n \tag{41}$$

for inner boundary turn.

$$\int_{-\infty}^{\infty}\left[v(\dot{w}'',t) - v(\dot{w}',t)\right]dw' = b(o+2)\ \frac{d}{dx} v_n - b^2\left[\frac{3p^2+2p+2}{2!} - A^{o*}\right]\frac{d^2}{dx^2} v_n$$

for outside bondary turn. (42)

If $p \geq 3$ and substituting w'' for x (43)

$$\int_{-\infty}^{\infty}\left[v(\dot{w}''t) - v(\dot{w}'t)\right] dw' = -\Bigg\{b(p+2)\ \frac{d}{d\dot{w}'} v_n + b^2\left[\frac{3p^2+2p+2}{2!} - A^*\right]\frac{d^2}{dw'^2} v_n$$

$$b^2(p-2)\left[(p^2+p+1)2 - A^*\right]\frac{d^2}{dw'^2} v_n - b(p+2)\ \frac{d}{dw'} v_n$$

$$b^2\left[\frac{3p^2+2o+2}{2!} - A^*\right]\frac{d^2}{dw'^2} v_n\Bigg\}$$

$$\int_{-\infty}^{\infty}\left[v(\dot{w}'',t) - v(\dot{w}',t)\right] d\dot{w}' = \left\{b^2(2p^3 + p^2 - 2 - A_o)\frac{d^2}{d\dot{w}'^2} v_n\right\} \quad (44)$$

where $A_o = 8p-4 \quad p \geq 3$

For the special case of a 2 layer coil

$$\int_{-\infty}^{\infty}\left[v(\dot{w}'',t) - v(\dot{w}',t)\right] d\dot{w}' = -14b^2 \frac{d^2}{d\dot{w}'^2} v_n \quad (45)$$

$$\therefore \int_{-\infty}^{\infty}\left[v(\dot{w}'',t) - v(\dot{w}',t)\right] d\dot{w}' = -Kb^2 \frac{d^2}{d\dot{w}'^2} v_n = K\left(\frac{\omega}{V}\right)^2 b^2 v \quad (46)$$

where K is given in Table 1.

TABLE I

Number of Layers	K
1	1
2	14
3	43
4	116
5	239
6	424
7	683
8	1028
9	1471
10	2024

A plot of K vs the number of layers appears in Figure 3.

Equations 1 and 2 then become for sinusoidal applied voltages as in equation 3.

$$j\frac{\omega V}{V} = ri + j\omega L\left(\frac{\omega}{V}\right) \quad (47)$$

$$j\frac{\omega i}{V} = Gv + j\omega\left(C_o + \frac{\omega^2 b\, K C_t}{V^2}\right) \quad (48)$$

These equations are those of an ordinary distributed constant line if

$$L = L\left(\frac{\omega}{V}\right) \quad (49)$$

$$C = C_o\left[1 + \left(\frac{\omega}{V}\right)^2 \frac{C_t\ Kb}{C_o}\right] \quad (50)$$

If the line is now assumed to be lossless, the well known solution of the transmission line equations of interest are:

time delay (per unit length) $T = \sqrt{LC}$ (sec/meter) (51)

phase shift $= \beta = \omega\sqrt{LC}$ (rad/meter) (52)

characteristic impedance $z_o = \sqrt{\frac{L}{C}}$ (ohms) (53)

Inserting equations (6), (49) and (50) in equation (51) we obtain

$$\left(\frac{T}{T_o}\right)^2 = 2I_1 \left(\frac{\pi D}{\lambda}\right) K_1 \left(\frac{\pi D}{\lambda}\right) \left[1 + \left(\frac{\omega}{V}\right)^2 \frac{C_t K_b}{C_o}\right] \quad (54)$$

where $T_o = \sqrt{L_o C_o}$, is the low frequency time delay. Substituting in equation (54) for $\frac{\omega}{V}$ we obtain

$$\left(\frac{T}{T_o}\right)^2 = 2I_1 \left(\frac{\pi D}{\lambda}\right) K_1 \left(\frac{\pi D}{\lambda}\right) \left[1 + q \left(\frac{\pi D}{\lambda}\right)^2\right], \quad (55)$$

where $q = \frac{4 C_t K_b}{C_o D^2}$ (56)

12. It is thus apparent that the stray capacitance between turns, C_t, is multiplied by a factor K. For a single layer line (K = 1) the effect of this capacitance is negligible. For a 3 or more layer line K has been increased many times and actually is large enough to compensate for the decrease of inductance with frequency as far as time delay is concerned. It is true that the characteristic impedance will suffer from this compensation, as it does with all other known compensation measures in delay lines. However the time delay is in general far more critical than characteristic impedance. This stray capacitance actually becomes our compensation and these lines are thus called self-compensated lines.

13. A plot of $\frac{T}{T_o}$ from equation (55) is shown in Figure 4. It will be observed that for a given delay line with $q > o$, $\frac{T}{T_o}$ decreases as the frequency increases to some minimum value and then increases without limit. If the maximum variation in time delay is prescribed q may be determined.

14. "If the variation from a linear phase characteristic is no more than 1/2 radian in a frequency range of $\frac{1}{3 \times \text{pulse length}}$

there will probably be no serious loss of signal detail."[8] "If the variation from a linear phase characteristic is as much as one radian in a frequency range of $\frac{1}{3 \times \text{pulse length}}$ complete loss of signal detail may be expected."[8] If a system is to pass pulses of duration T the approximate bandwidth is made[8]

$$F = \frac{1}{2T}. \qquad (57)$$

From the above, however, we require that the deviation from linearity in 2/3 of the bandwidth given by equation (57) shall not be more than 1/2 radian.

15. Thus, if a pulse whose duration was 0.166 microsecond was to be passed, the phase distortion would have to be less than 1/2 radian up to 2 megacycles. This corresponds to a total error in time delay ($T-T_o$) of 0.04 microseconds. Thus, if the total delay was 1 microsecond the error could be 4%.

16. Let us arbitrarily allow the $\frac{T}{T_o}$ curve to go as much above 1, for a given value of q, as the curve did go below 1. Thus, from Figure 4, we can secure the % variation in time delay vs q. This curve appears as Figure 5. Thus, in the example of the last paragraph q must be greater than 0.35. Figure 6 is a plot of % variation in time delay vs $\left(\frac{\pi D}{\lambda}\right)_{max}$. The value of was obtained from Figure 4 where the T/T_o curve crosses the maximum error in T allowable in upward direction. Figure 7 shows $\left(\frac{\pi D}{\lambda}\right)_{max}$ vs q from Figures 5 and 6.

17. The variation in time delay of these multilayer self-compensated lines are very similar to single layer lines with compensation patches[9].

18. The design equations of multilayer lines may now be stated.

Rewriting equation (56) as

$$C_o = \frac{4C_t K_e b}{D^2 q}, \qquad \text{farads/meter,} \qquad (58)$$

and using $C_t = \frac{\pi^2 D K_e \varepsilon_o}{\sqrt{2}} \sqrt{\frac{a}{b-a}}$ farads, (59)

where K_e is the relative dielectric constant of the insulation on the wire, we finally get

$$C_o = \frac{4\pi^2 K_e \varepsilon_o K b}{D\sqrt{2}\, q} \sqrt{\frac{a}{b-a}} \qquad \text{farads/meter.} \qquad (60)$$

This is a convenient form to relate the compensation capacitance (C_t) to the capacitance to ground (C_o) as we have equations to

relate to C_o to the physical dimensions of the line.

$$C_o = \frac{2\pi K_{ed} \varepsilon_o}{\ln D_1/D_2} \quad \text{farads/meter,} \qquad (61)$$

where K_{ed} is the dielectric constant of the insulation between the core and the winding,
D_2 is the core diameter,
and D_1 is the diameter of the core plus the insulation.

19. This simple formula is applicable in most multilayer lines, but it should be noted that there is a capacitance formed by the insulation on the wire itself. As the dielectric constants are not, in general, the same, more exact results may be secured by considering both mediums[10]. In most cases however equation (61) is accurate enough.

20. The inductance of a long solenoid is given by the well known expression

$$L_o = \frac{\pi N^2 D^2 \mu_o}{4} \quad \text{(henries/meter),} \qquad (62)$$

where N is the number of turns per meter.

21. From Figure 4 it is obvious that some variation in time delay is unavoidable. This variation in time delay is a variation in phase response (see equations (51) and (52)). It is well known that any variations in the amplitude or phase response of a system will alter the wave form of the output signal of the systems. From the method of paired echoes[11] we know that amplitude distortion produces distortion symmetrical about the center of the pulse, while phase distortion produces anti-symmetrical distortion of the pulse. The response of a unit impulse passed through several kinds of amplitude distortion is shown in Figure 8. From some measurements made on the amplitude distortion of these lines with sinusoidal signals applied, it appears that the response of these lines resembles (c) through much of the range with a sharper drop at some higher frequency where the amplitude is already very low.

22. The phase distortion of an uncompensated and self-compensated line is shown in Figure 9. The phase distortion approaches the form indicated in Figure 10. The response to a unit impulse is also shown in Figure 10 if the phase error is assumed sinusoidal. The response is altered by the echo or impulse overshoot. The magnitude[11] of this echo is

$$= \frac{J_1(\Delta\beta)}{J_2(\Delta\beta)} , \qquad (63)$$

where J_1 is the Bessel Function of the first kind and 1st order, J_0 is the Bessel Function of the first kind and 0th order.

23. It is thus apparent that the amplitude distortion produces symmetrical overshoot echoes and phase distortion produces anti-symmetrical overshoot echoes. Measurements of amplitude and phase distortion echoes on typical lines used in this report are shown in Table II. This table demonstrates that phase distortion is causing most of the overshoot in most of the lines wound.

24. Thus with the aid of equations (51), (53), (60), (61), (62), (57) and statement below equation (57), and Figures 3, 4 and 5 this type of line may be designed. Lines have been wound when the average number of layers was not an integer. In this case the value of K was read from Figure 3 for the average number of layers. No difference in performance of these lines has been noticed.

25. In general lines have been bank wound with layers from 2 through 5 and wire sizes from 32 through 47 with several kinds of insulation. These lines have had impedances from 2,000 ohms through 10,000 ohms and time delays from 2.5 to over 30 microseconds per meter. Examples are given in Table II. Experimental evidence to substantiate the theory developed in this section will be given.

Line Construction

26. The lines were wound on 3/16 inch diameter polystyrene cores 12 inches long. These cores were given several coats of silver conducting paint to form the ground strip. Although the cores could be slotted after an overnight drying period a much cleaner cut was made if the drying period was several days. The cores were axially slotted forming 36 thin strips, each strip being about 0.015 inch wide. The slots were about 0.003 inch wide. A one inch length of the core was left unslotted to facilitate the connection of the external ground lead. The core was covered with a layer of insulating material to give the required winding-to-core capacitance. A piece of thin teflon tape was wound around the core. A number of small pieces of scotch cellophane tape held the teflon on the core until the line was wound. The scotch tape was removed piece by piece as the line was wound.

27. The winding was done on a lathe. In order to provide uniform wire tension, both to secure a good winding and to prevent breakage, a wire feeding device was used. The wire feeding device and the slotting device are shown in Figure 11. The wire tension was adjustable over a range of about 10 to 70 grams. The tension was continuously indicated by a pointer.

28. A wire guide attached to the longitudinal feed of the lathe was placed about 1/16 inch from the core, which was chucked in the lathe. The longitudinal travel of the wire guide could be as low as 0.00066 inch per turn. As this distance is a fraction of the wire diameter, the result was a multiple layered coil approximating a bank winding. The far end of the core was attached to a counter chucked in the tail-stock. A steel drill rod was inserted through a hole in the core for rigidity. A 10 inch long winding was wound on the core. Lines have been wound with speeds varying from about 200 to 800 rpm.

29. A magnified view of the end of the line showing details of construction appears in Figure 12.

Measurements

30. The method for determining the characteristic impedance of these delay lines was based upon the fact that no reflections occur in an idealized delay line terminated in characteristic impedance. The value of the characteristic impedance in a practical case involving complex waves must therefore be compromised for minimum reflections over the band of frequencies for which the line is designed to operate. The lines were terminated at the input as well as the output to minimize any possible secondary reflections at the input. A suitable means of determining the effective characteristic impedance when the line is used to delay rectangular pulses is to feed the pulse itself into the delay line and to adjust the terminating impedances for minimum reflections. A block diagram illustrating the experimental method for determining the characteristic impedance of these delay lines and for recording the response of the delay lines to rectangular pulses appears in Figure 13. The pulse generator was of the delay line type. RG-65/U delay line cable was used. This pulse generator was triggered by a Lavoie type LA-592A pulse generator. A Hewlett Packard type 212A pulse generator was used on occasion in observing the response of the lines to pulses of greater than 1 microsecond duration. A Tektronix type 517 oscilloscope was used. The oscilloscope sweep was triggered by the input pulse. A camera, mounted on the oscilloscope, was used to record the input and output wave shapes of the delay line. A video amplifier was placed between the delay line and the pulse generator. The load impedance of the video amplifier was made equal to the characteristic impedance of the line. A diagram of the video amplifier appears in Figure 14.

31. The pulse distortion and attenuation were also measured with the same equipment. The oscilloscope camera was used to record the wave forms of both the input and output signals and the measurements were made directly from the photographs as the sweep of the type 517 oscilloscope is quite linear and the sweep time in milli-microseconds per centimeter quite accurate.

32. The vertical gain was kept constant for both input and output pulses so that attenuation measurements could be made from the photographs.

33. The delay time as well as the rise time and fall time was likewise measured on the oscilloscope. The delay time was defined as the time between the mid-point of the leading edge of the input and output wave forms. The rise and fall times were defined as the time duration between the 10% and 90% values of the pulse amplitude. The pulse duration was defined as the time between the 50% values. The attenuation was measured by comparing the amplitudes of the input and output pulses.

34. Although the pulse response of the lines was used as a measure of their ability, some sinusoidal data were taken. In order to determine the validity of the equations, a line was connected to a r.f. signal generator through a 10,000 ohm resistor as shown in Figure 15. The Tektronix 517 oscilloscope was used as a VTVM. With the line short circuited, the frequencies at which the impedance of the line was a minimum, was noted. The line was thus electrically $\frac{\lambda}{2}$, $\frac{2\lambda}{2}$ etc. long. The measurements were repeated with the line open circuited, the line then being $\frac{\lambda}{4}$, $\frac{3\lambda}{4}$, $\frac{5\lambda}{4}$ etc. long electrically. From this data, the measured values of L_o and C_o at low frequencies, and the physical dimensions of the line, $\frac{\pi D}{\lambda}$ could be calculated.

Experimental Results

35. Photographs of the input and output wave forms for several short lines appear in Figure 16. All input pulses are 1 microsecond duration. Line A has an average of 4.7 layers of AWG 41F wire and was 1.65 inches long with a delay of 1.03 microseconds. This line had a bad reflection occurring near the middle of the line as can be observed. Line B has 4 layers of AWG 41F wire and was 2.44 inches long with a delay of 0.6 microsecond. Line C has 3 layers of AWG 39F wire and was 2-3/4 inches long and had a delay of 1.17 microseconds. The last row of photographs are the input and output wave forms observed using a 15 foot piece of RG-65/U cable which had a delay of 0.7 microsecond. The gain of the scope was kept constant in each line so that the attenuation in the lines may be observed.

36. Photographs of the input, output and input and output wave forms superimposed for another line appear in Figure 17. Line D has 3 layers of AWG 41HF wire and was 9.75 inches long. It had a delay of 2.1 microseconds. In the photograph of input and output wave forms superimposed some small variations are observed in the base line. Those not originating with the pulse itself (due to finite passband and compensation limitations) probably occur due to minor reflections from discontinuities in the line.

Reflections of this magnitude are present in most of the lines wound. For comparison purposes the response of a 46 foot piece of RG-65/U cable is shown as well as a 3 foot piece of General Electric 1100 ohm cable.

37. Examples of lines wound with other insulated wires appear in Figure 18. All these lines are wound with 3 layers of AWG 41 wire with different types of insulation. Line F was wound with heavy formex insulation ($K_e = 3.1$). Line F was wound with Sprague Electric Company Ceroc ST insulation (assumed $K_e = 3$). This wire has an inorganic ceramic insulating coating thinly deposited on copper wire with an overlay of teflon. Line G was wound with Sprague Electric Company Ceroc 200 insulation (assumed $K_e = 3$). This wire has an overlay of silicon instead of teflon but otherwise the same as Ceroc ST. Line H is a teflon insulated wire ($K_e = 2$) of Hitemp Wires, Incorporated. In general the characteristics of all these lines are similar. Due to the lower dielectric constant of the teflon, line H has a higher characteristic impedance and a shorter delay per unit length.

38. Lines have been wound with size AWG 47 wire. The pulse response of such a line appears in Figure 19. It will be noted that the attenuation for this line is considerably greater than those previously mentioned. This is due to the increased ohmic resistance of this very small wire. Extreme care had to be used in winding lines with this small wire.

39. The response of a higher impedance line is shown in Figure 20. This line had characteristic impedance of 10,000 ohms. The response of another line to pulses of various durations is shown in Figure 21.

40. An attempt was made to check Figure 4 by the method outlined in section IV. The measurements made on line C is shown in Figure 22. The crosses indicate open circuit measurements and the circles indicate short circuit measurements; a comparison of Figure 22 and Figure 4 indicates that q is about 0.4. From measurements of capacity to ground the value of q was found to be 0.605. The error is considered to be well within experimental limits when one considers that there was no means of accurately placing each turn in accordance with the geometrical pattern assumed in the theoretical derivation. Measurements were also made on several other lines and the discrepancy of these lines was about the same as the one shown.

41. Characteristics of a line with longer delay are shown in Figure 23. This line was 35-1/2 inches long and had a delay of 7.35 microseconds. As a comparison a 112 foot section of RG-65/U cable is shown. This cable had a delay of 5.8 microseconds. It is apparent that the rise time of this line is considerably better than that of RG-65/U cable even though its delay is considerably longer. Several bad reflections are apparent due to wire breakage and improper winding.

42. The rise times of several of the lines which were more or less identical have been plotted in Figure 24. The data points on curve are indicated with crosses. The data points for RG-65/U cable are indicated by circles. From this curve it is apparent that the rise time of self-compensated lines and RG-65/U cable are about equal at a delay time of about 3.5 microseconds and at longer delays the self-compensated line is considerably better.

43. More data on the lines shown in all the photographs appears in Table II. The cut-off frequency is computed from the rise time[11].

$$F_c = \frac{0.445}{T_r} \tag{64}$$

CONCLUSIONS

44. Experimental evidence has shown good agreement with the theoretical analysis within experimental error.

45. It is observed that these multilayer self-compensated, bank wound lines have considerably longer delays per axial inch, have considerably reduced attenuations for the same delay time, but suffer from more internal reflections. For short delays (up to about 2 microseconds) the rise time is considerably poorer. This, of course, means lower cut-off frequencies. At delays of greater than 4 microseconds, however, the rise time is considerably better than RG-65/U. This is attributed to the fact that the output pulse of these lines remains largely unchanged as the time delay increases, while RG-65/U cable has an exponential rise and fall with a flat top.

46. Experimental evidence indicates little variation of attenuation with different wire insulating materials. A higher dielectric constant material on the wire would give increased compensation and thus give even greater delays per unit length.

47. It appears that the attenuation of these lines can be reduced somewhat and fewer minor reflections obtained if a better winding technique can be developed to approach more closely a true bank wound line.

	Dia(in)	Average No. of Layers of Winding	Length(in)	Time lay/inch	f_o mc	Measured Overshoot Due to Amplitude Distortion	Measured Overshoot Due to Phase Distortion
Line A	3/16	4.7	1.65	0.63	4.4	6%	1.4%
Line B	"	4	2.44	0.45	4.2	6%	1%
Line C	"	3	2.75	0.22	6.8	6%	12%
Line D	"	3	9.75	0.20	2.7	5%	15%
Line E	"	3	5.3	0.21	3.2	6%	12%
Line F	"	3	9.9	4±0.20	2.8	6%	13%
Line G	"	3	10.0	4±0.19	2.9	7%	16%
Line H	"	3	10.0	4±0.17	3.2	8%	18%
Line I	"	2.4	10.0	0.34	3.0	2%	12%
Line J	1/4	3.5	9.3	0.48	2.02	8%	1%
Line K	3/16	3	10.0	0.38	3.75	17%	3%
Line L	"	3	35.5	0.21	1.9	1%	9%
RG-65/U			180	0.0043	8.8		
RG-65/U			552	0.0043	3.75		
RG-65/U			1344	0.0043	1.5		
GE			36	0.047	5.5		

	Dia(in)	Average No. of Layers of Winding	Length(in)	Wire	Z_o Measured	Z_o Calculated from 1000 Cycle Measurements of L & C	T(usec) Measured	T(usec) Calculated from 1000 Cycle Measurements of L & C	Rise Time of Line Measured	q Measured
Line A	3/16	4.7	1.65	41F	3955	3572	1.03	1.035	0.1	0.94
Line B	"	4	2.44	39F	3925	3545	1.2	1.17	0.11	0.72
Line C	"	3	2.75	41F	2647	2673	0.6	.597	0.07	0.6
Line D	"	3	9.75	41HF	3927	4070	2.1	1.935	0.17	0.62
Line E	"	3	5.3	41HF	3955	3830	1.25	1.12	0.14	0.55
Line F	"	3	9.9	41 Ceroc ST	4290	4250	2.05	1.97	0.16	0.65
Line G	"	3	10.0	41 Ceroc 200	4290	4150	2.15	1.93	0.15	0.7
Line H	"	3	10.0	41 Teflon	4750	4755	1.75	1.73	0.14	0.57
Line I	"	2.4	10.0	47HF	5600	6800	3.2	3.17	0.15	0.15
Line J	1/4	3.5	9.3	44F	10,000	9500	4.5	4.3	0.22	0.7
Line K	3/16	3	10.0	46HF	5600	5820	3.8	3.8	0.12	0.23
Line L	"	3	35.5	41HF	3740	3750	7.6	7.35	0.24	0.55
RG-65/U			180		1000		.78		0.05	
RG-65/U			552		1000		2.4		0.12	
RG-65/U			1344		1000		5.8		0.3	
GE			36		1100		1.7		0.08	

TABLE II

Z_o Measured	Z_o Calculated from 1000 Cycle Measurements of L & C	T(usec) Measured	T(usec) Calculated from 1000 Cycle Measurements of L & C	Rise Time of Line Measured	q Measured	Attenuation DB	Attenuation DB/usec	Time Delay/inch	f_o mc	Measured Overshoot Due to Amplitude Distortion	Measured Overshoot Due to Phase Distortion
3955	3572	1.03	1.035	0.1	0.94			0.63	4.4	6%	1.4%
3925	3545	1.2	1.17	0.11	0.72			0.45	4.2	6%	1%
2647	2673	0.6	.597	0.07	0.6			0.22	6.8	6%	12%
3927	4070	2.1	1.935	0.17	0.62	0.81	0.39	0.20	2.7	5%	15%
3955	3830	1.25	1.12	0.14	0.55	0.72	0.58	0.21	3.2	6%	12%
4290	4250	2.05	1.97	0.16	0.65	0.76	0.37	0.20	2.8	6%	13%
4290	4150	2.15	1.93	0.15	0.7	0.72	0.33	0.19	2.9	7%	16%
4750	4755	1.75	1.73	0.14	0.57	0.52	0.3	0.17	3.2	8%	18%
5600	6800	3.2	3.17	0.15	0.15	4.15	1.3	0.34	3.0	2%	12%
9,000	9500	4.5	4.3	0.22	0.7	0.9	0.2	0.48	2.02	8%	1%
5600	5820	3.8	3.8	0.12	0.23	1.45	0.4	0.38	3.75	17%	3%
3740	3750	7.6	7.35	0.24	0.55	1.6	0.22	0.21	1.9	1%	9%
1000		.78		0.05		1.68	0.7	0.0043	8.8		
1000		2.4		0.12		3.3	0.57	0.0043	3.75		
1000		5.8		0.3		1.38	0.8	0.0043	1.5		
100		1.7		0.08				0.047	5.5		

NAVORD Report 3759

2

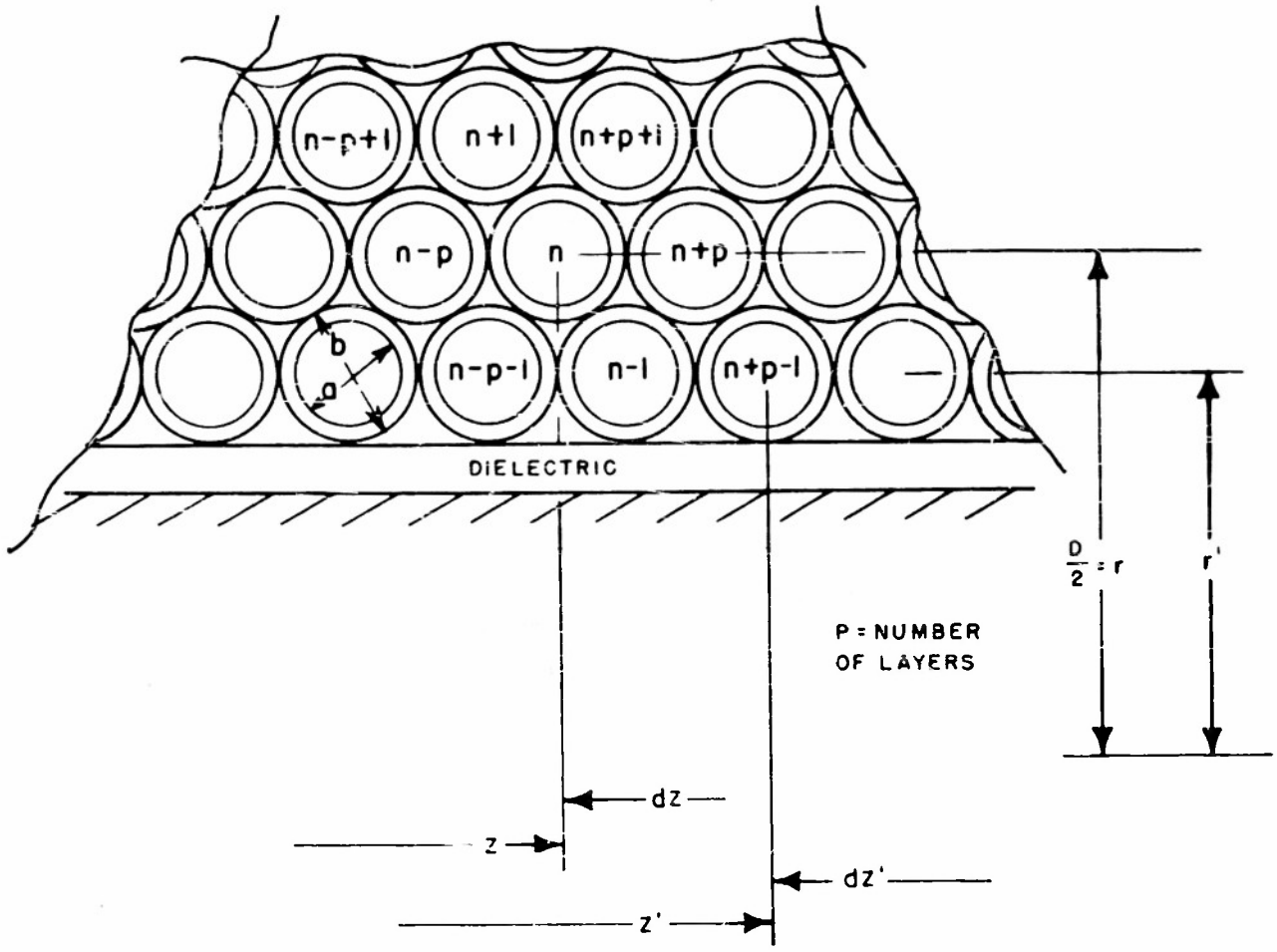

FIG. 1 CROSS SECTION OF LINE

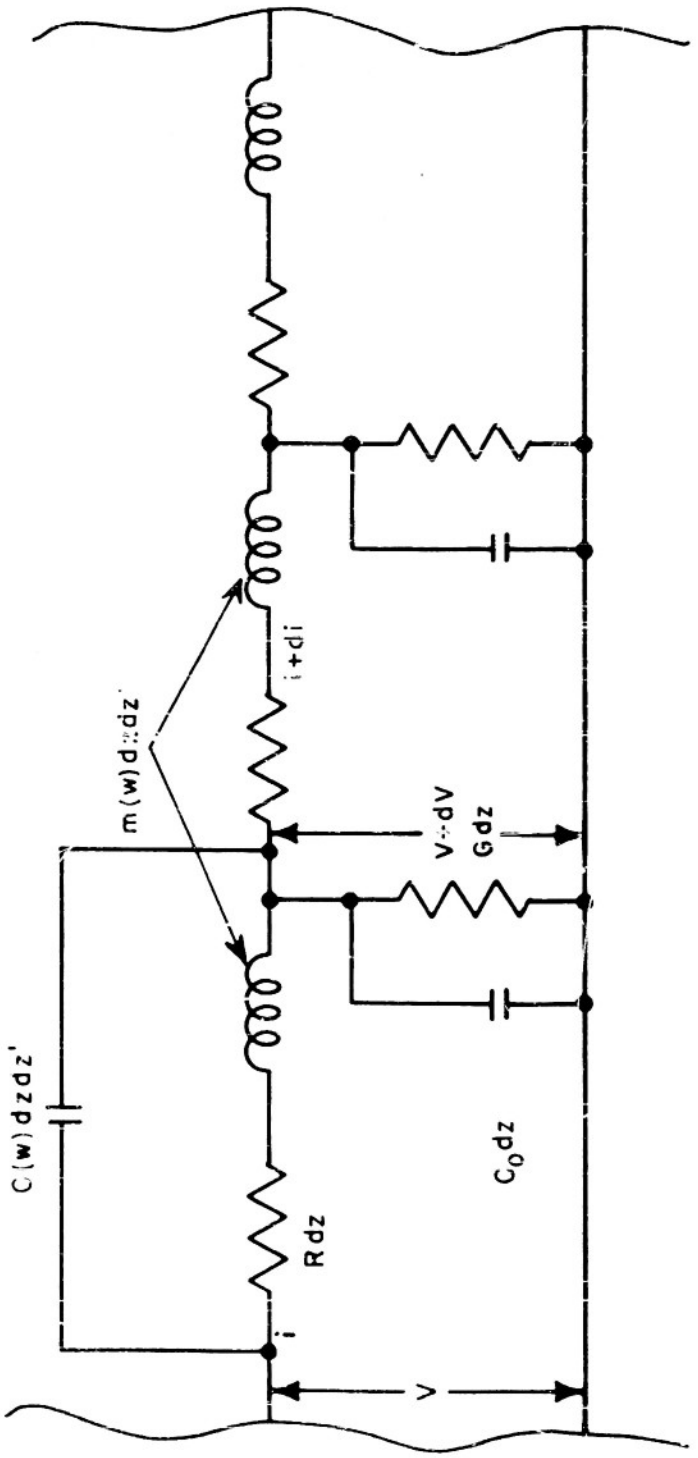

FIG. 2 SCHEMATIC DIAGRAM OF A SECTION OF LINE

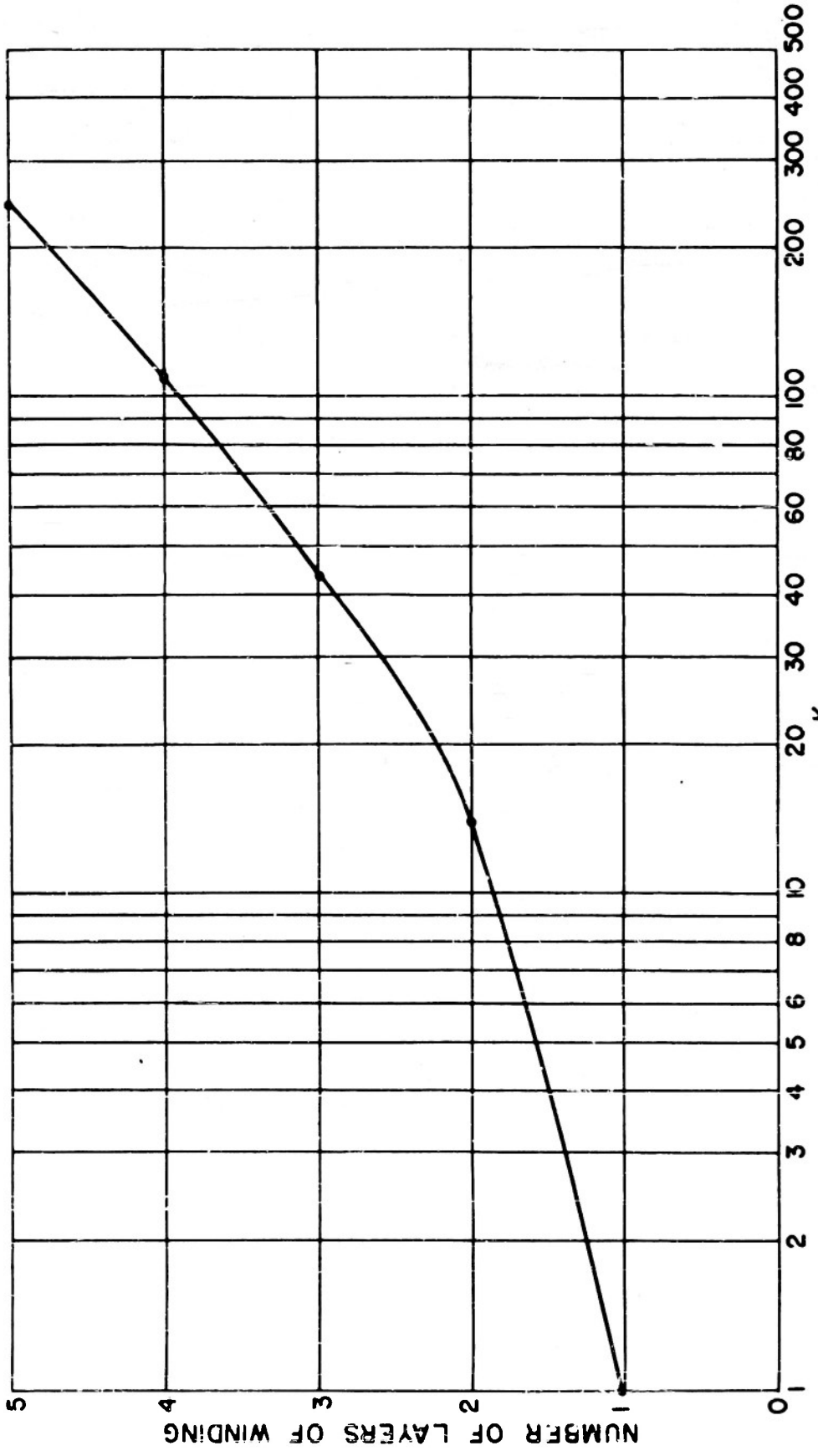

FIG. 3 NUMBER OF LAYERS OF MULTILAYER BANK WINDING VS K

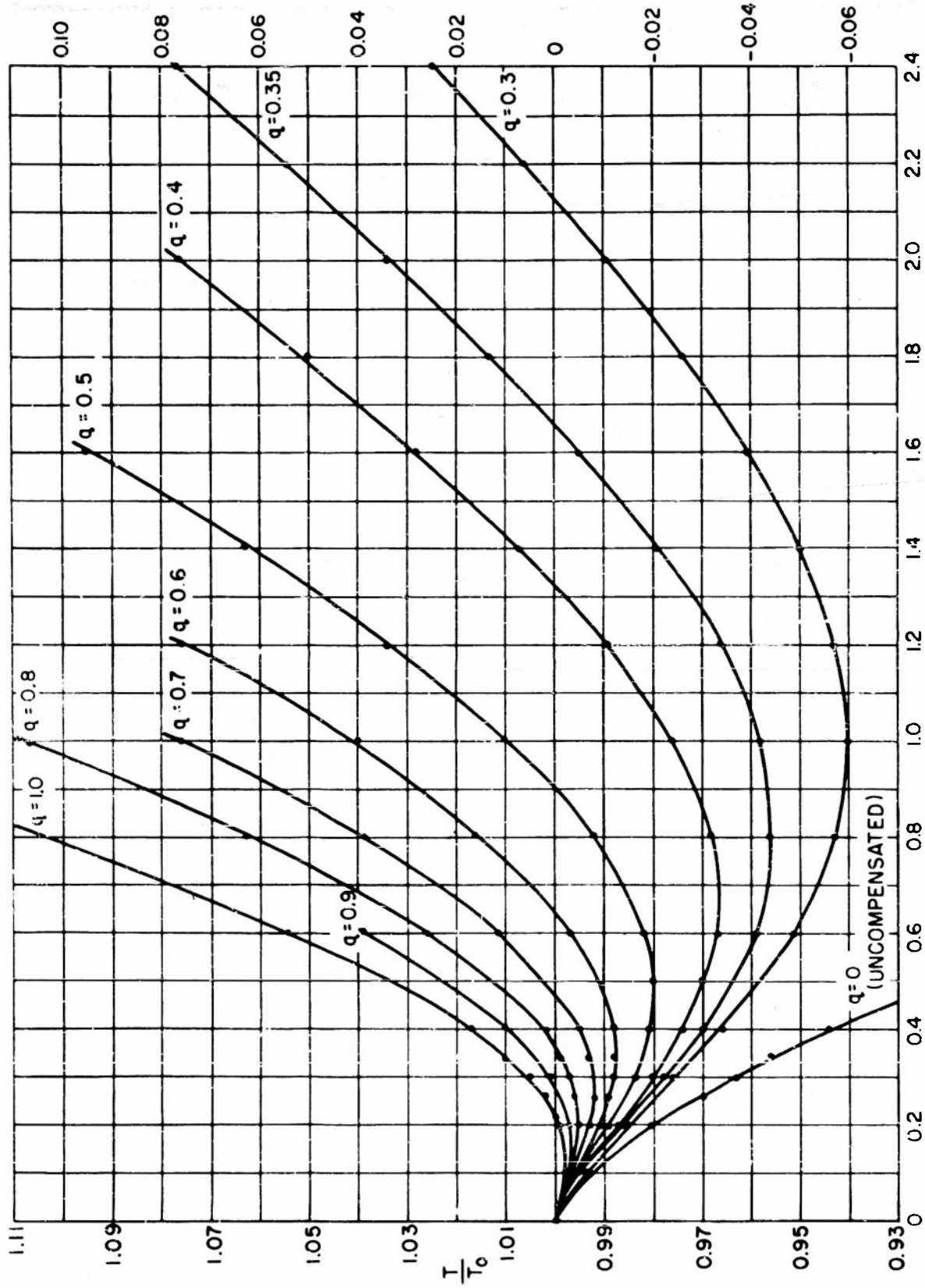

FIG. 4 $\frac{T}{T_0}$ VS $\frac{\pi D}{\lambda}$ FOR VARIOUS VALUES OF q

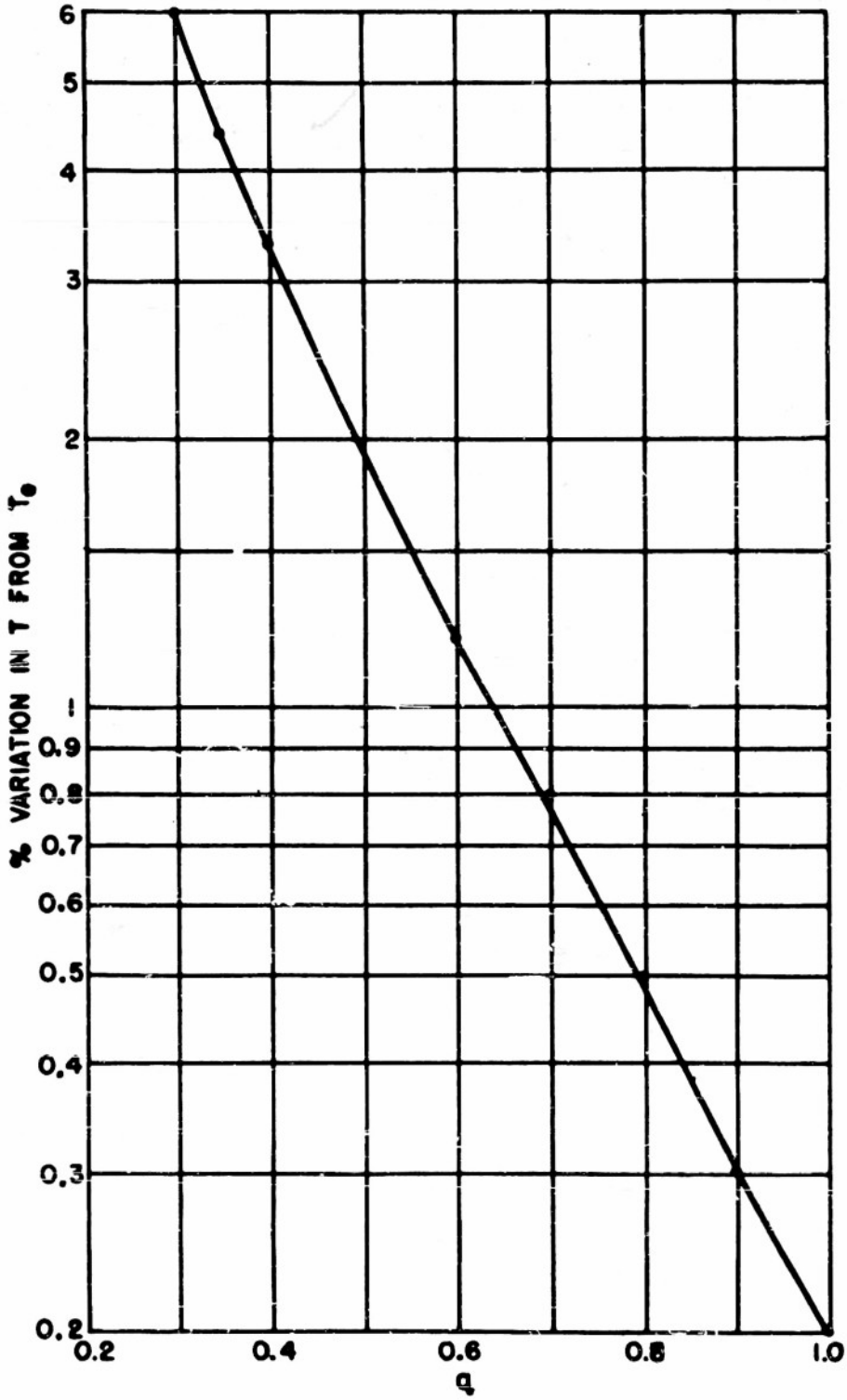

FIG. 5 % VARIATION IN T VS q

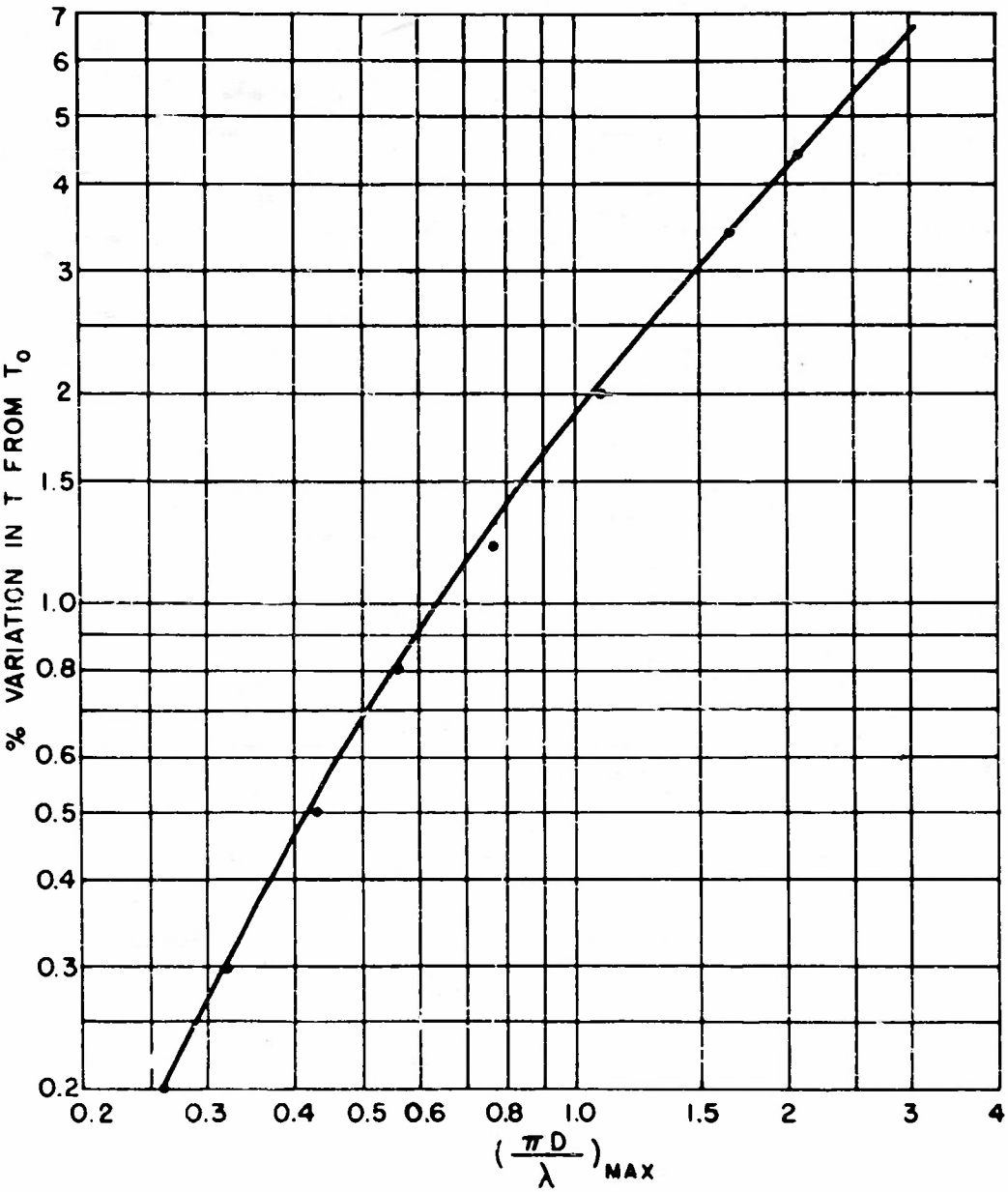

FIG. 6 % VARIATION IN T VS $(\frac{\pi D}{\lambda})_{MAX}$

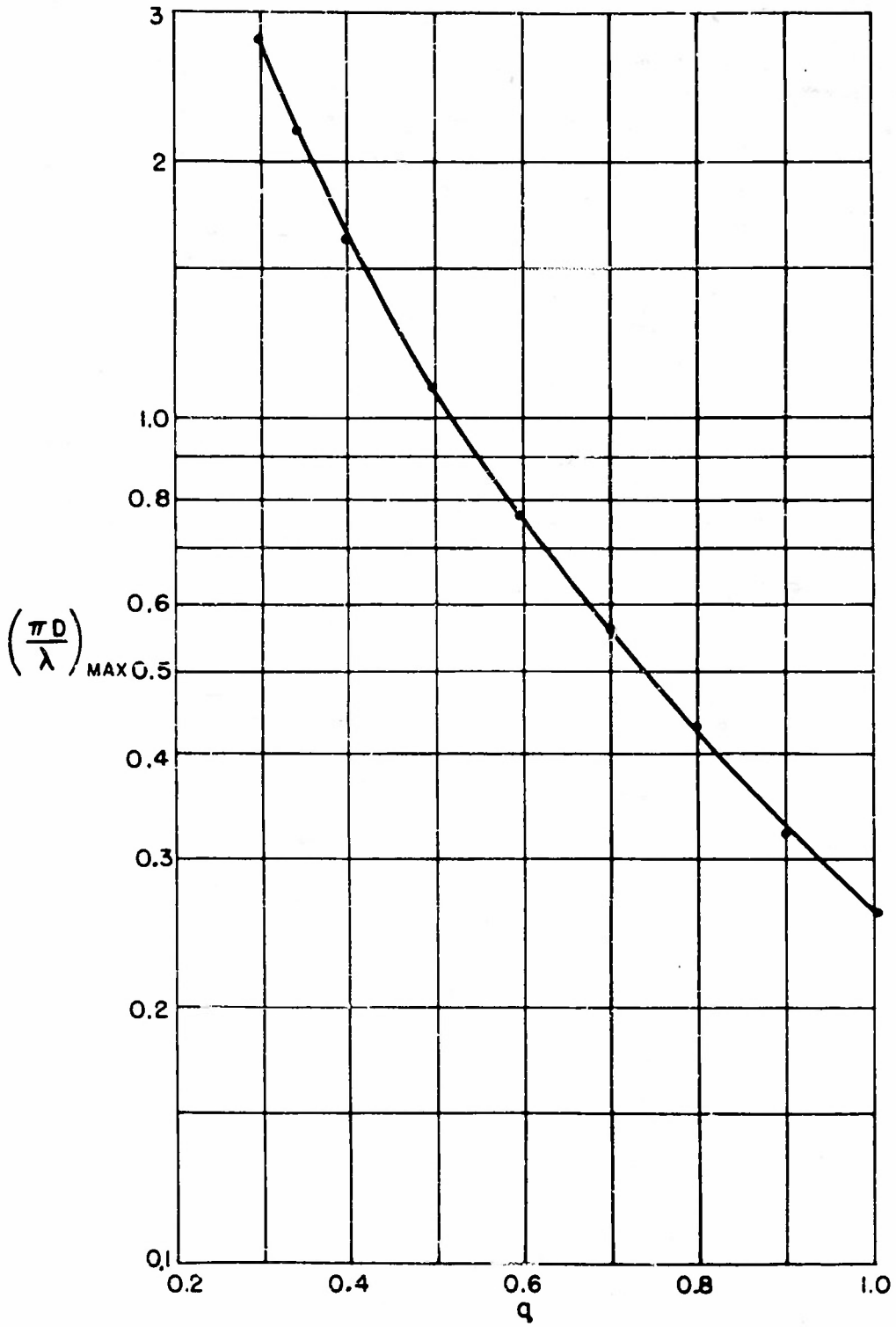

FIG. 7 $\left(\frac{\pi D}{\lambda}\right)_{MAX}$ VS q

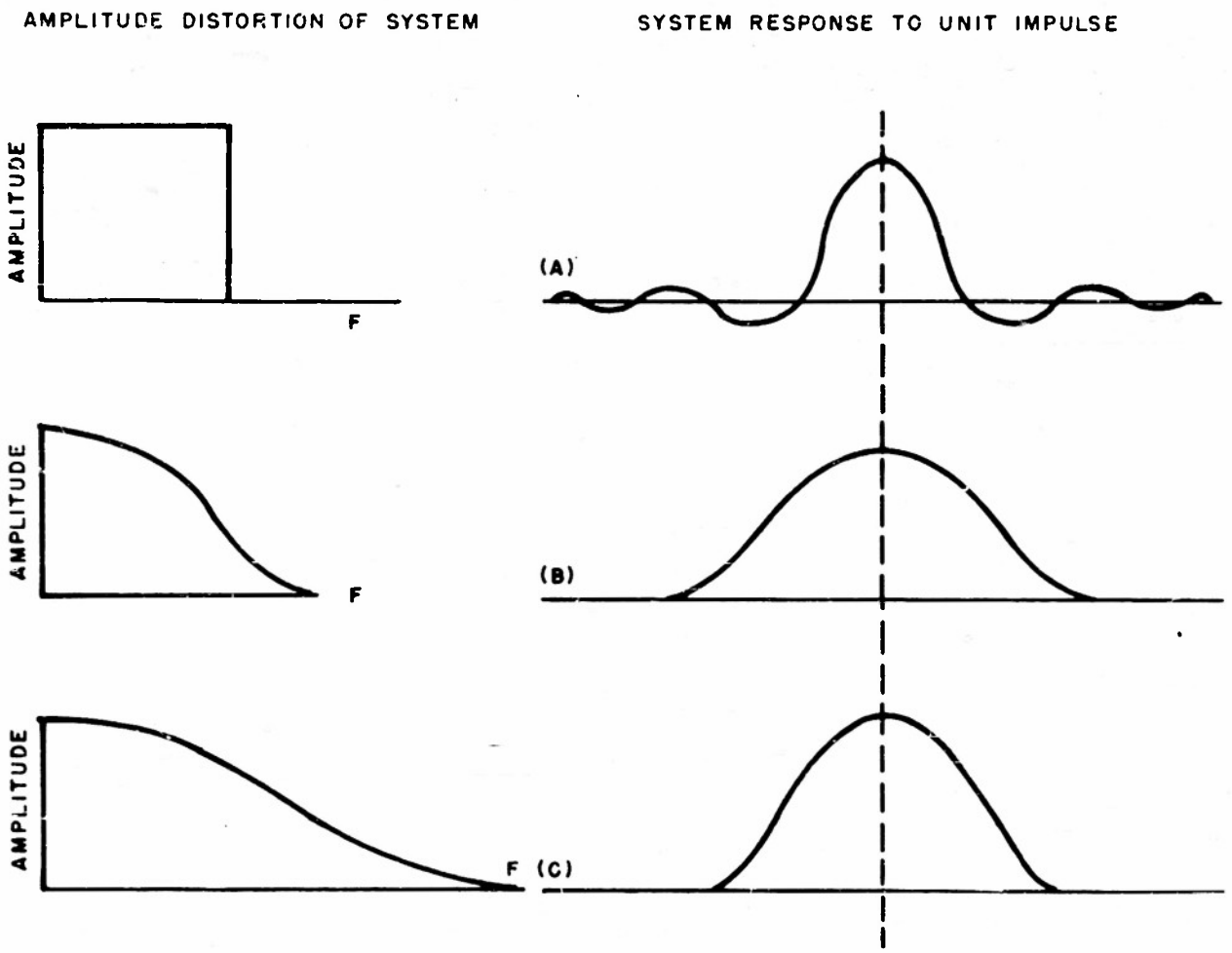

FIG. 8 EFFECTS OF AMPLITUDE DISTORTION WITH NO PHASE DISTORTION ON THE RESPONSE TO A UNIT IMPULSE

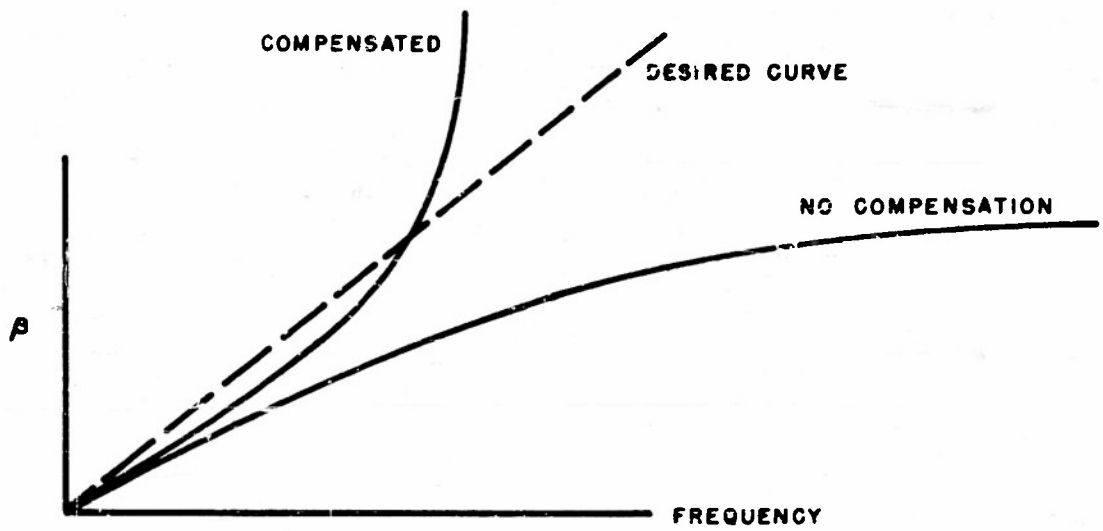

FIG. 9 PHASE SHIFT vs FREQUENCY

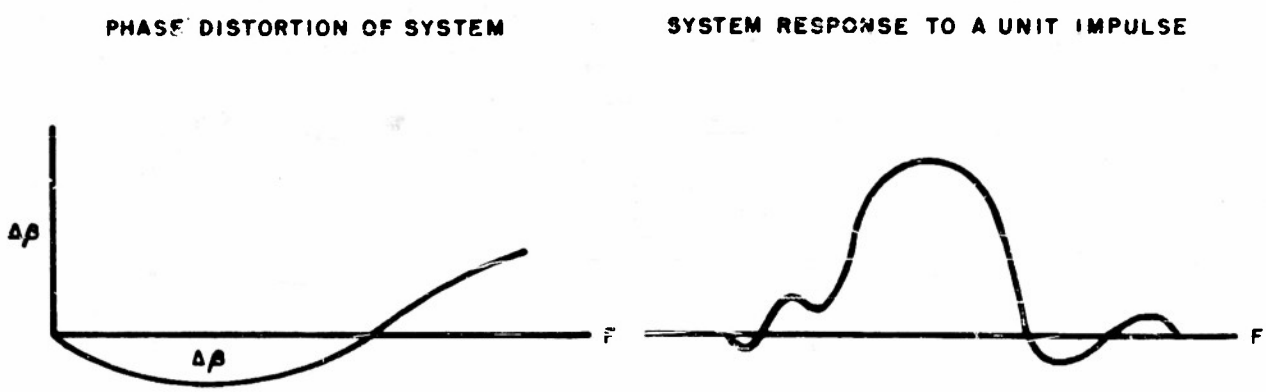

FIG. 10 EFFECTS OF A SINUSOIDAL PHASE DISTORTION WITH NO AMPLITUDE DISTORTION ON THE RESPONSE TO A UNIT IMPULSE

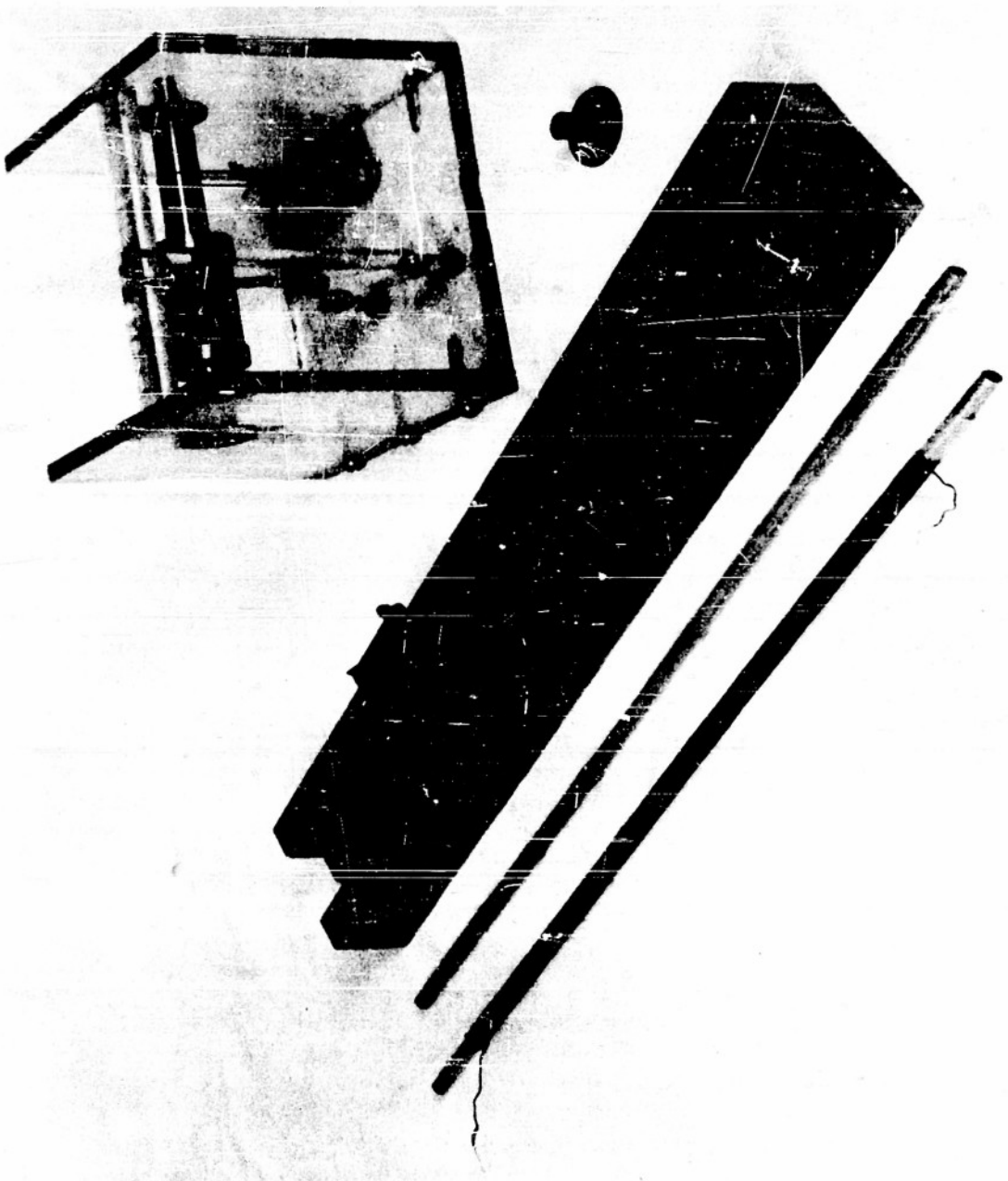

FIG. 11 WOUND DELAY LINE, SLOTTED CORE, SLOTTING EQUIPMENT, AND WIRE FEEDING DEVICE

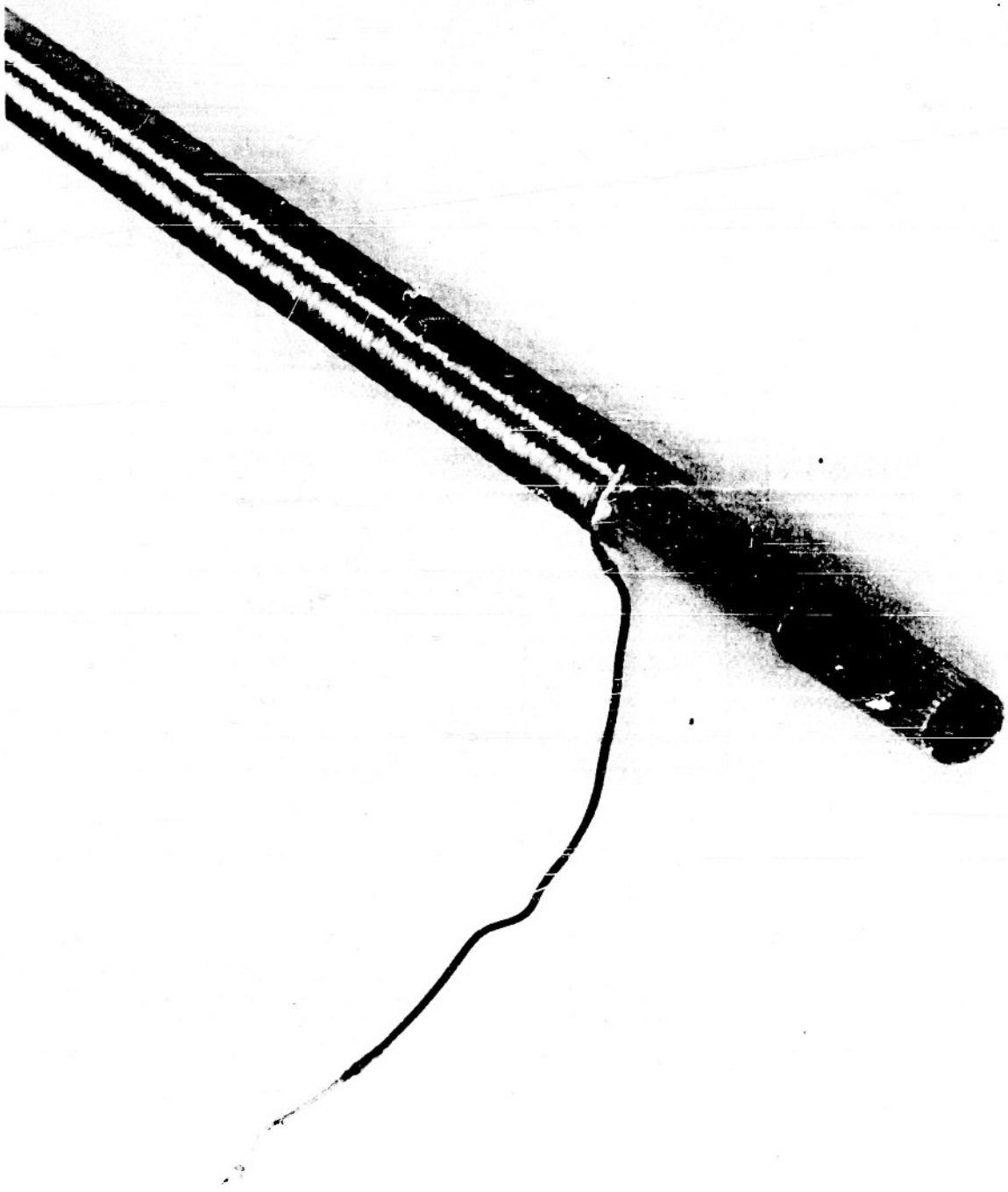

FIG. 12 END PORTION OF A BANK WOUND LINE

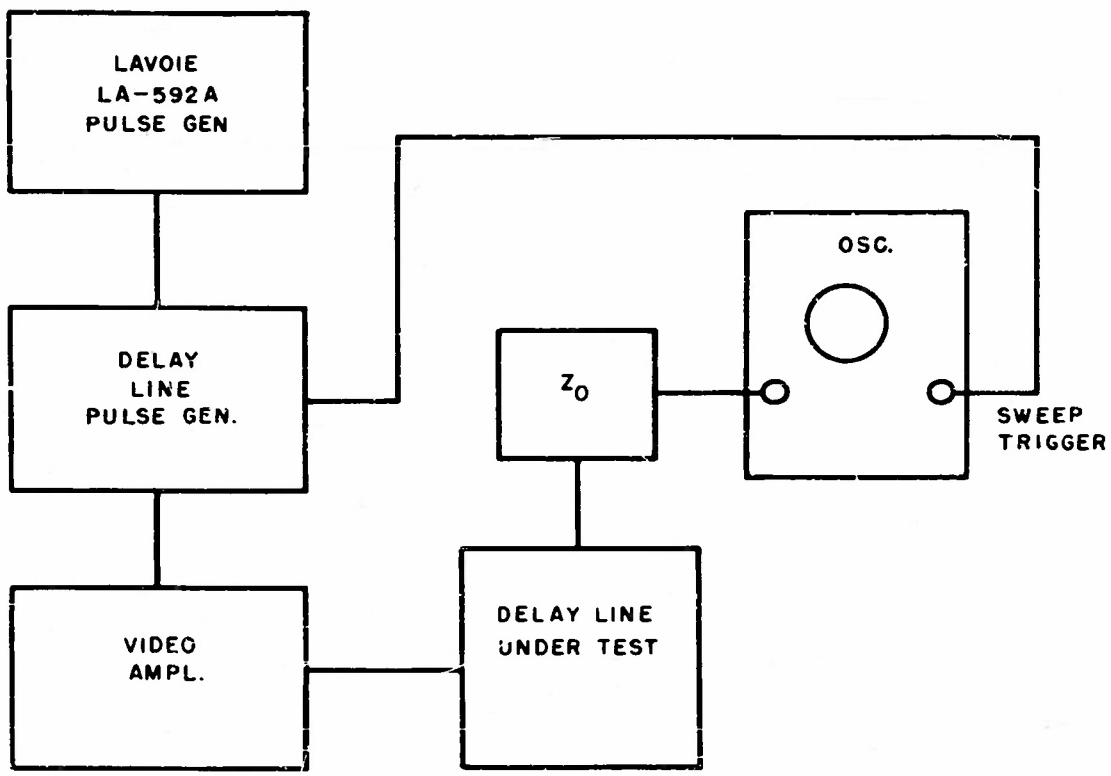

FIG. 13 BLOCK DIAGRAM OF MEASURING EQUIPMENT

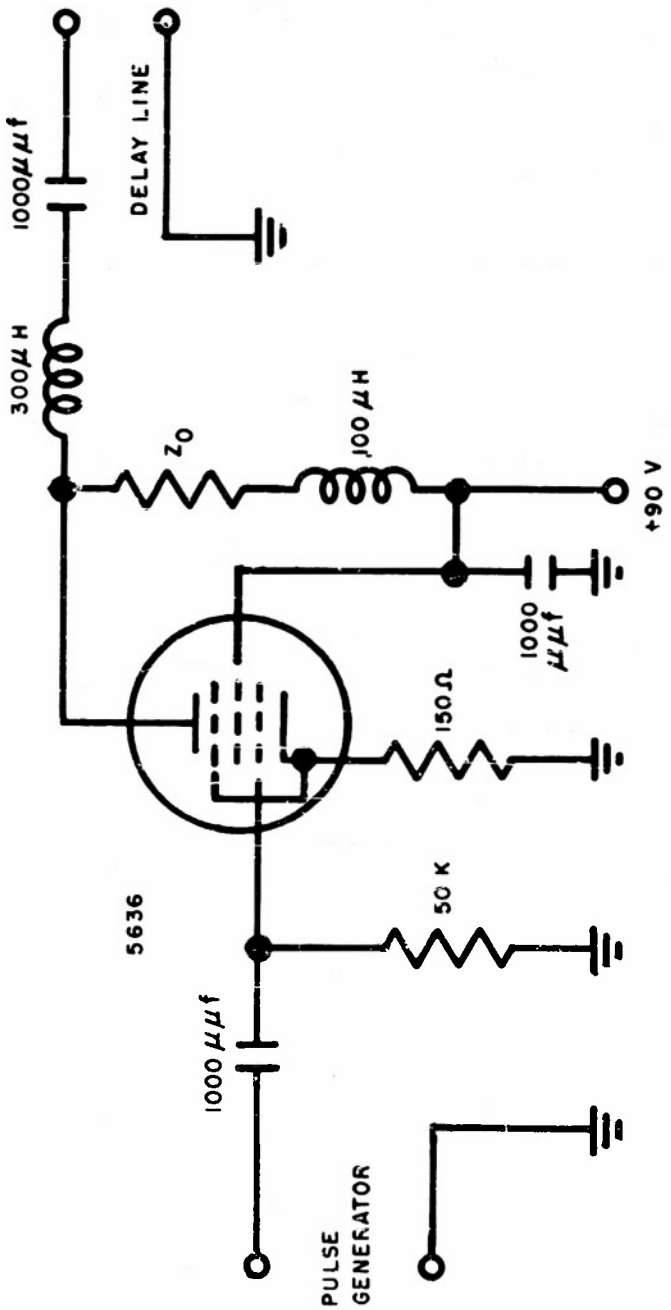

FIG. 14 VIDEO AMPLIFIER CIRCUIT DIAGRAM

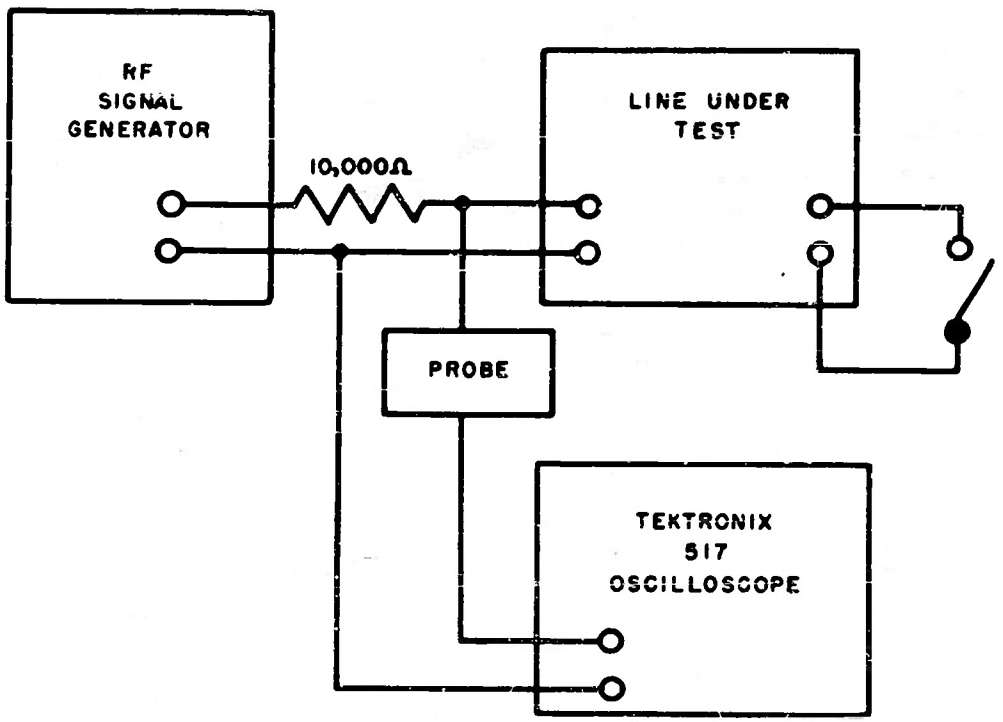

FIG. 15 BLOCK DIAGRAM OF EQUIPMENT
FOR OPEN AND SHORT CIRCUIT DATA

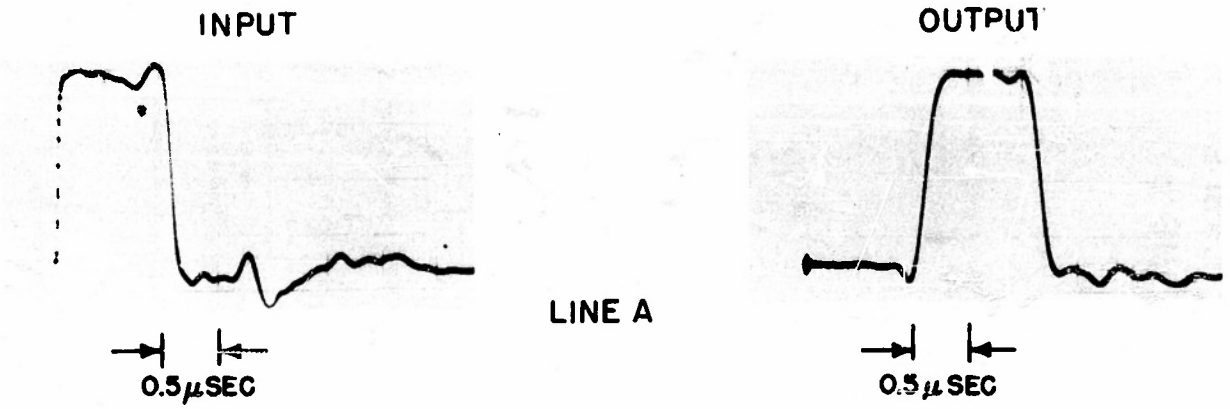

1.65 IN. LONG, 4.7 LAYER BANK WOUND LINE USING 41 FORMEX INSULATED WIRE (TOTAL DELAY 1.03 μSEC)

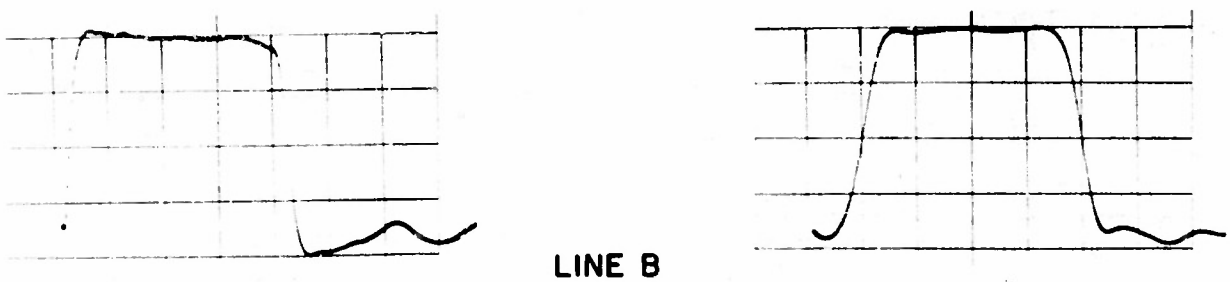

2.44 IN. LONG 4 LAYER BANK WOUND LINE USING 41FORMEX INSULATED WIRE (TOTAL DELAY 1.17 μSEC)

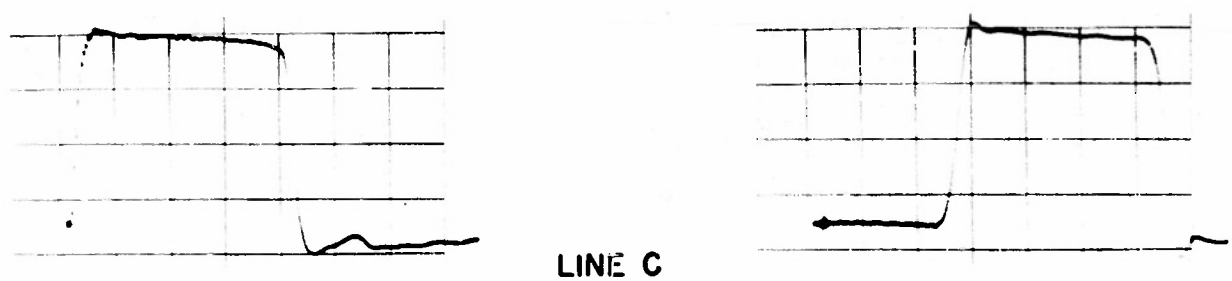

2.75 IN. LONG 3 LAYER BANK WOUND LINE USING 39F FORMEX INSULATED WIRE (TOTAL DELAY 0.6 μSEC)

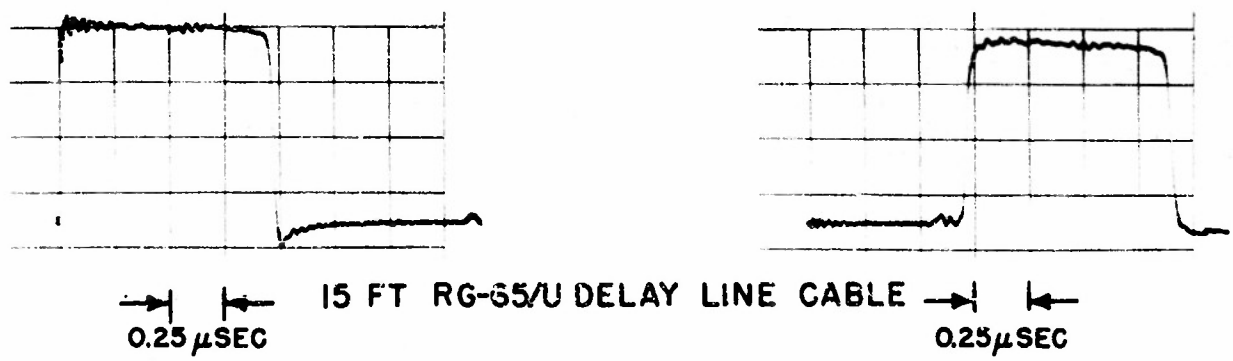

FIG. 16 PULSE RESPONSE OF SEVERAL BANK WOUND LINES AND A SHORT LENGTH OF RG-65/U DELAY LINE CABLE

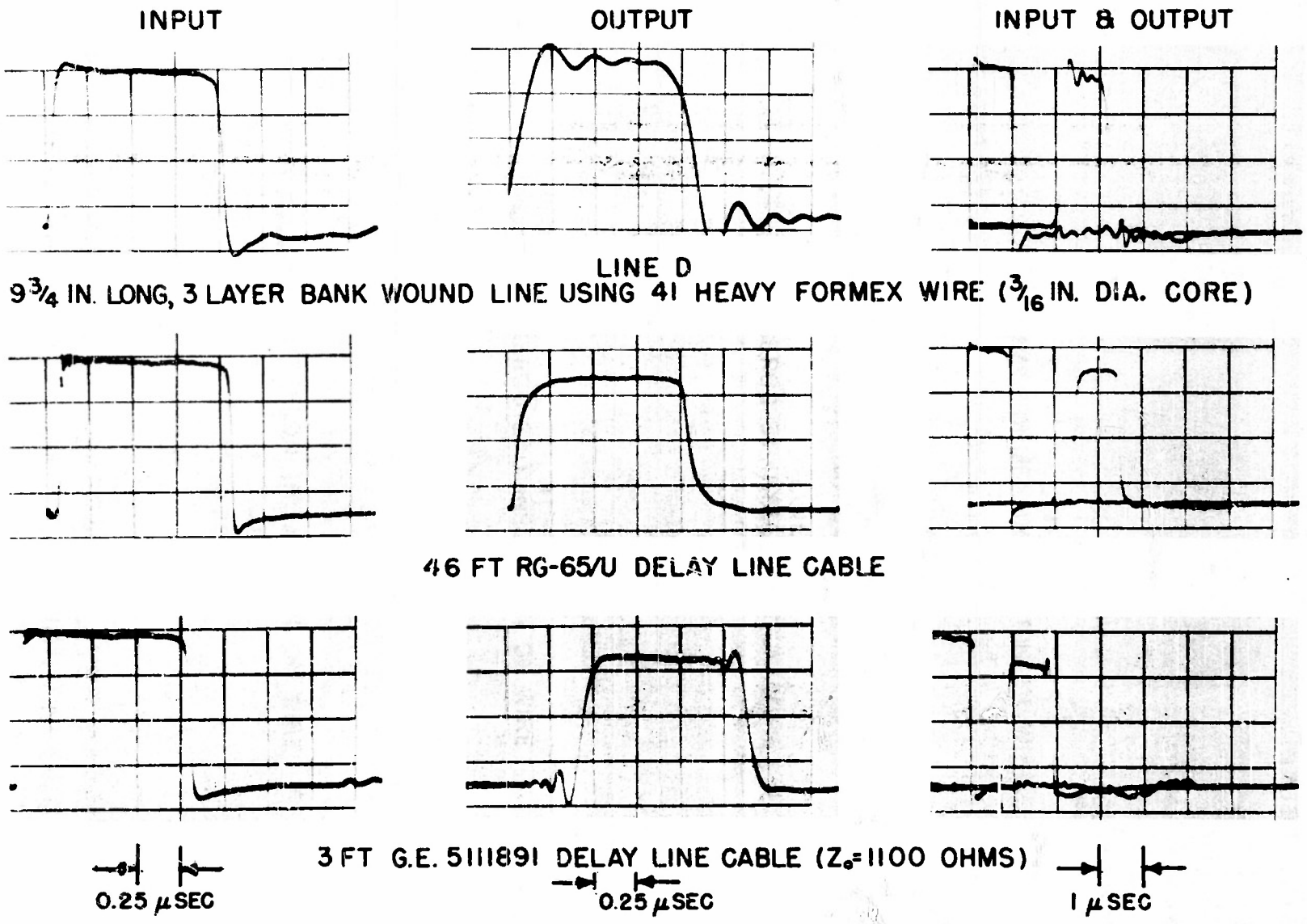

FIG. 17 COMPARISON OF PULSE RESPONSE OF A BANK WOUND LINE WITH RG-65/U DELAY LINE CABLE AND G.E. 5111891 DELAY LINE CABLE

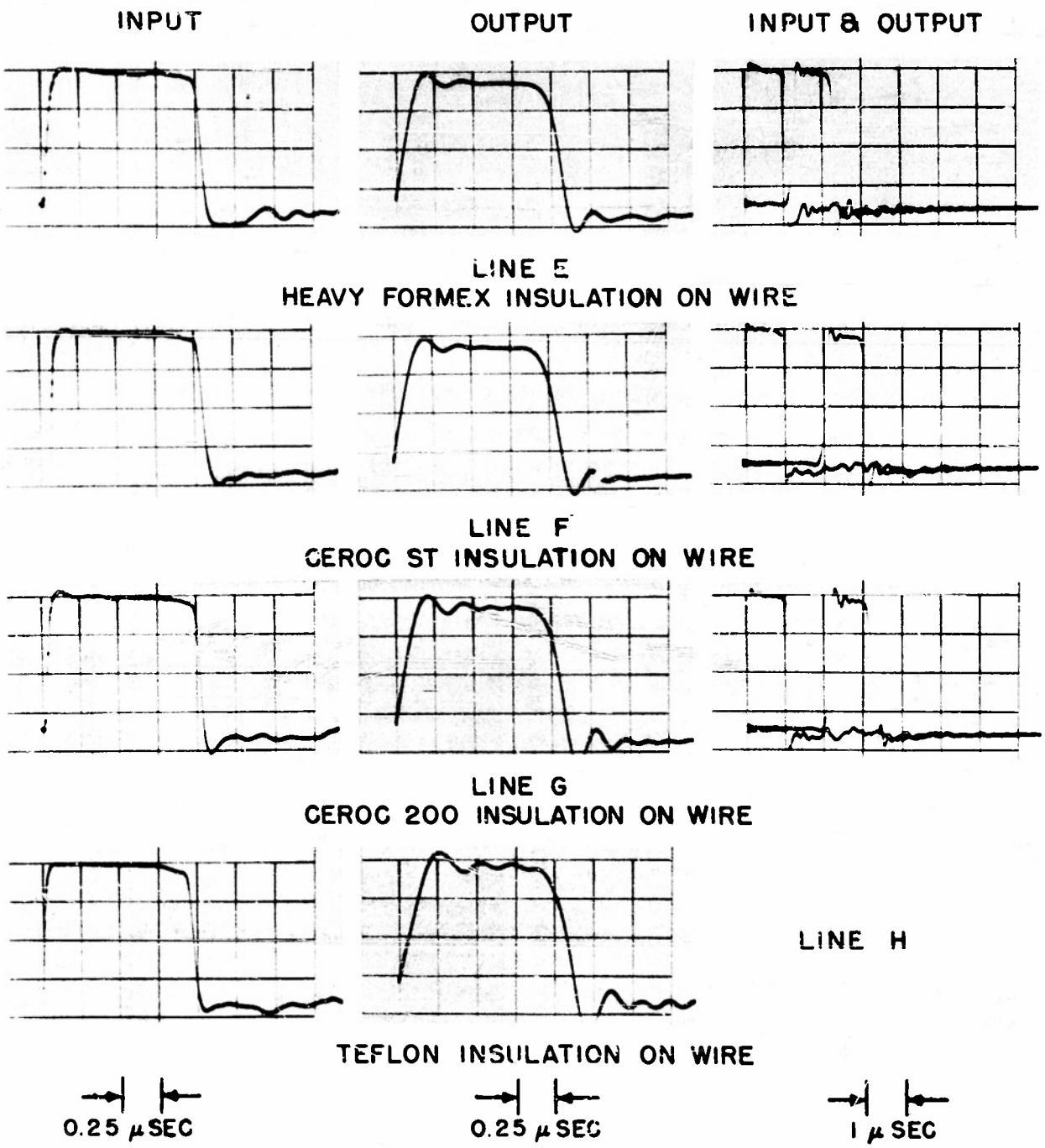

FIG. 18 COMPARISON OF SEVERAL 3 LAYER BANK WOUND LINES FOR VARIOUS TYPES OF INSULATION ON A.W.G. 41 WIRE

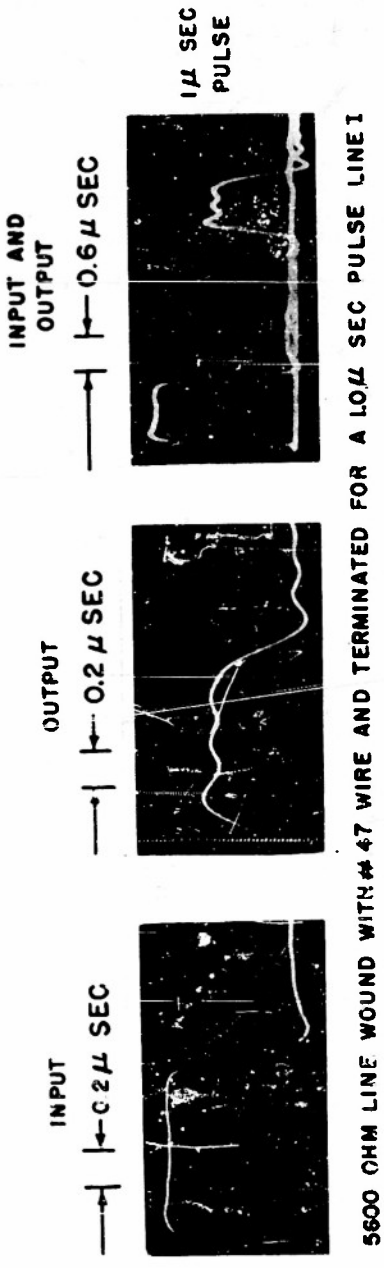

FIG. 19 PULSE RESPONSE OF A LINE WOUND WITH A.W.G.# 47 WIRE

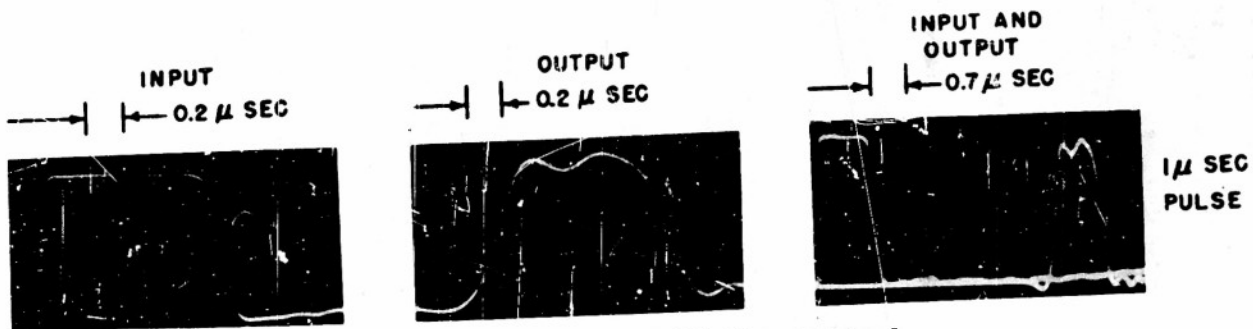

LINE ABOVE TERMINATED IN A 10,000 OHM RESISTOR
LINE J

FIG. 20 PULSE RESPONSE OF A 10,000 OHM LINE

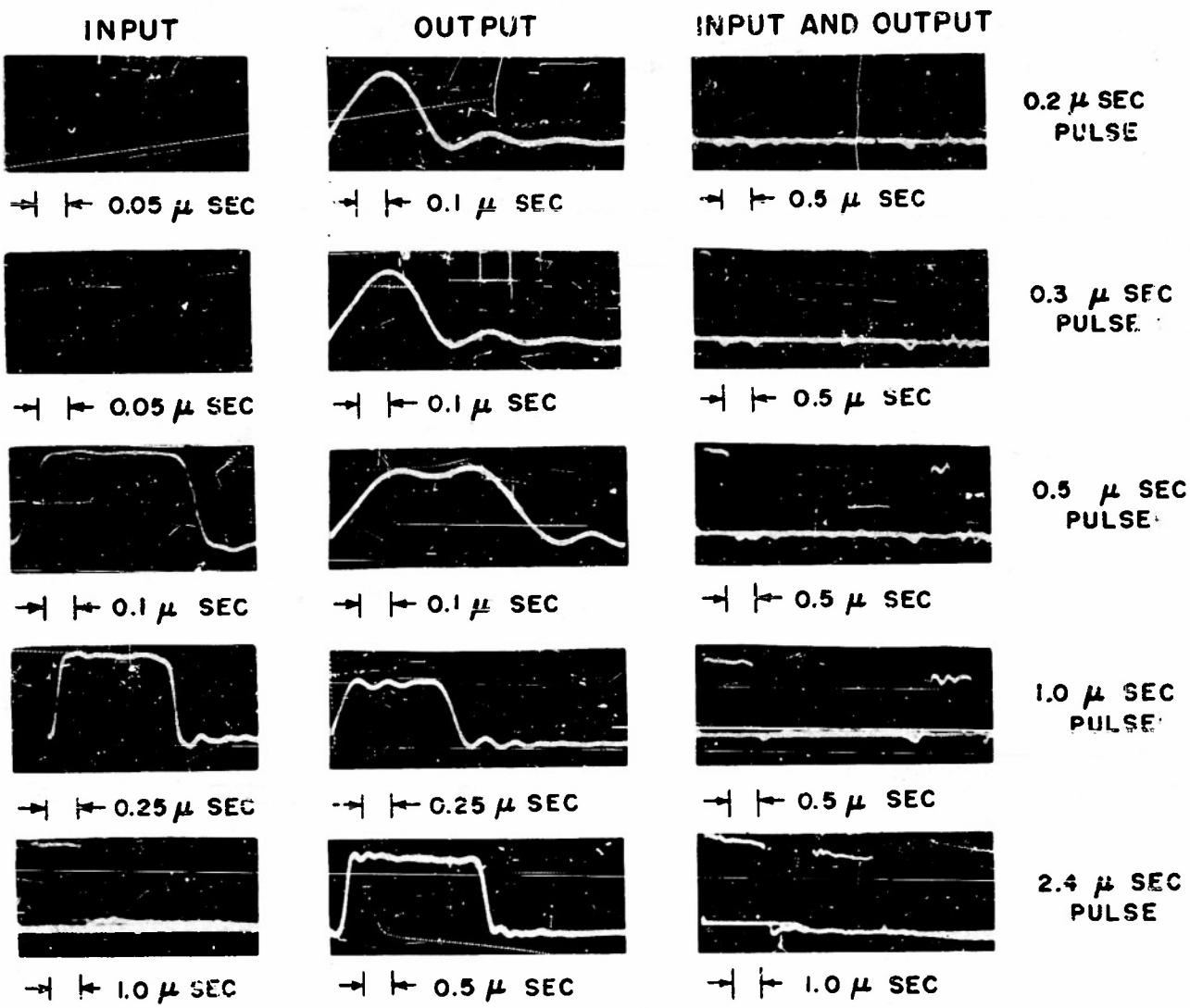

FIG. 21 PULSE RESPONSE OF A LINE TO VARIOUS PULSE DURATIONS

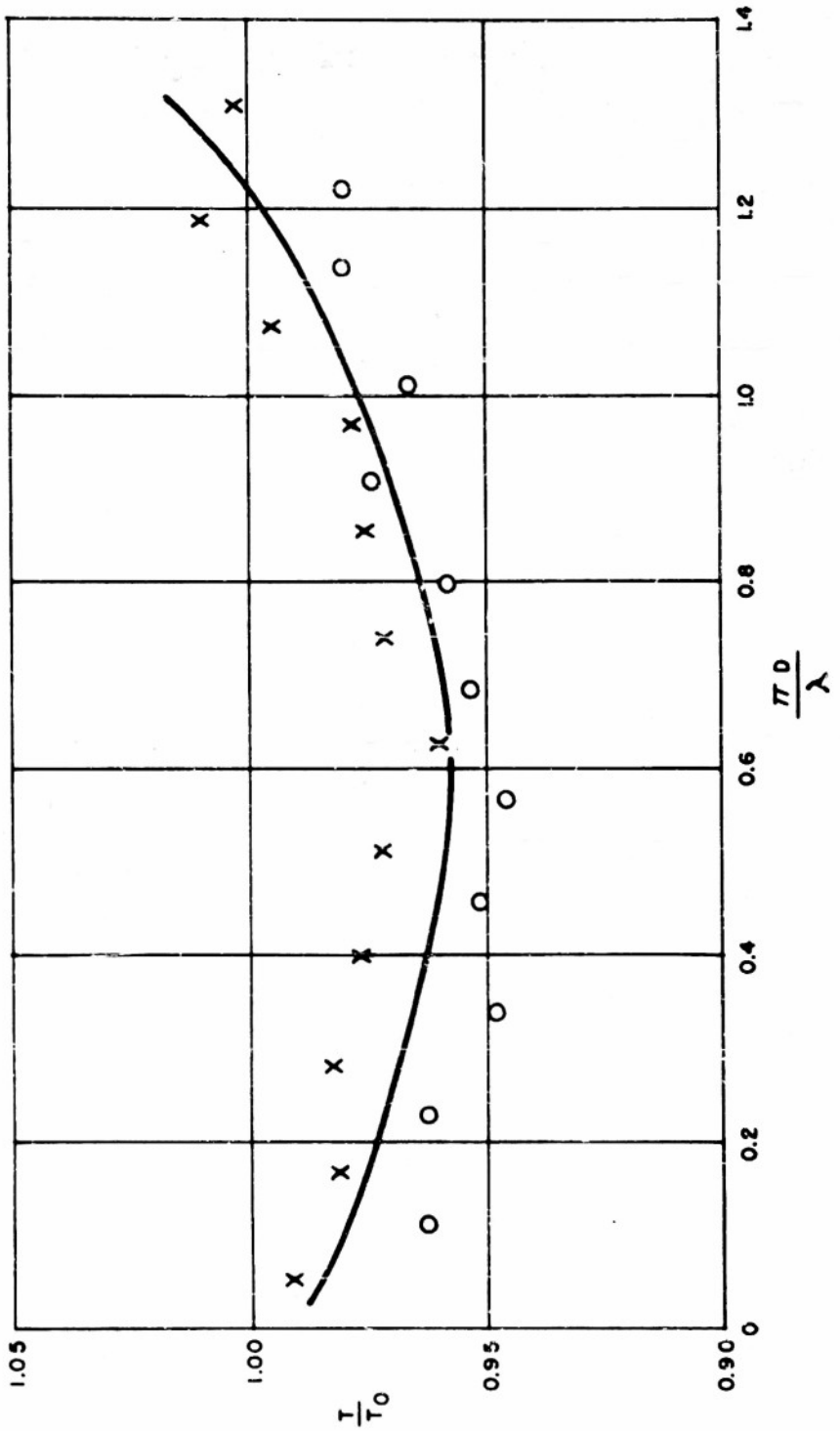

FIG. 22 A PLOT OF $\frac{T}{T_0}$ vs $\frac{\pi D}{\lambda}$ FOR A TYPICAL LINE (LINE C)

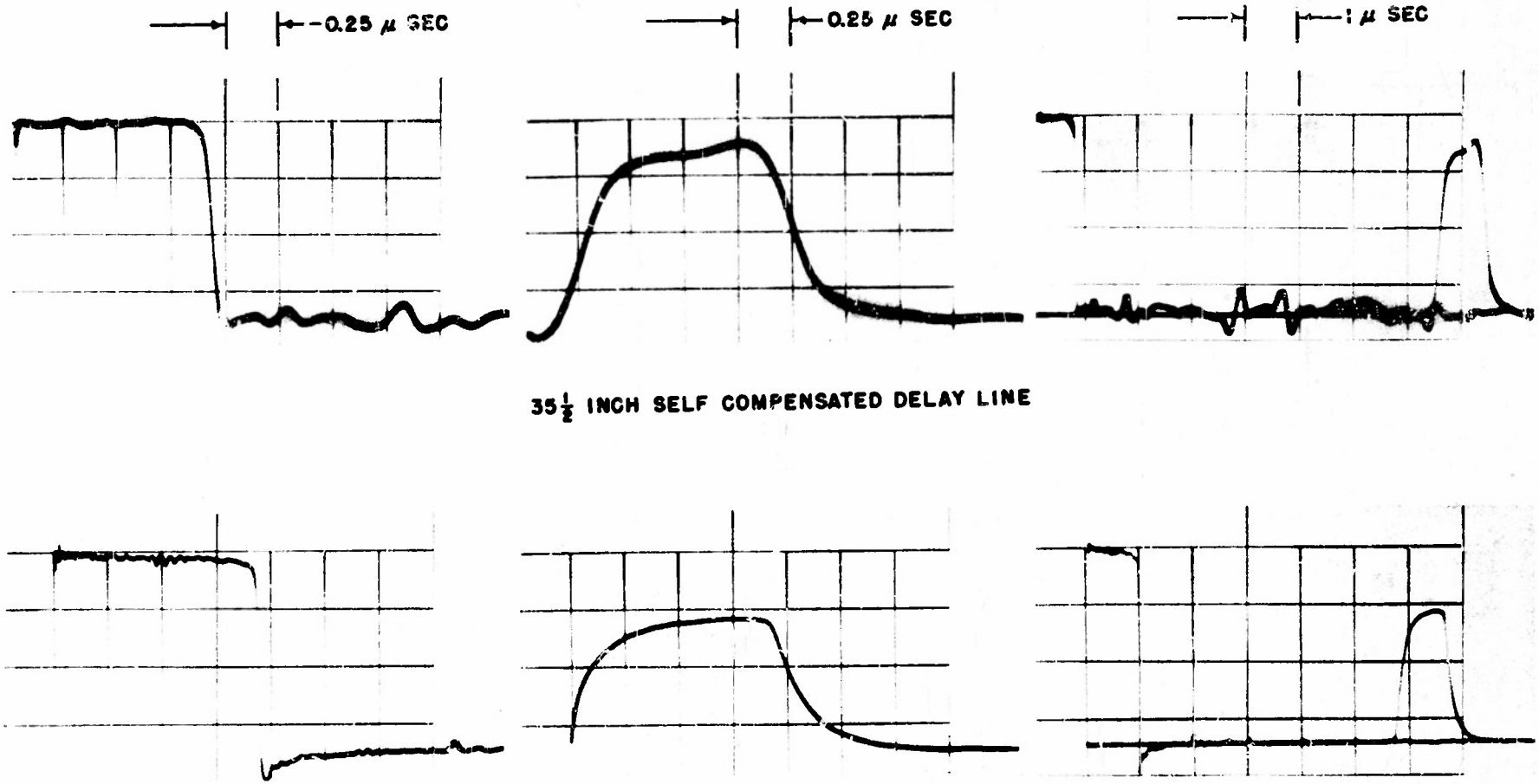

FIG. 23 COMPARISON OF PULSE RESPONSE OF A LONG BANK WOUND LINE WITH RG-65/U DELAY LINE CABLE

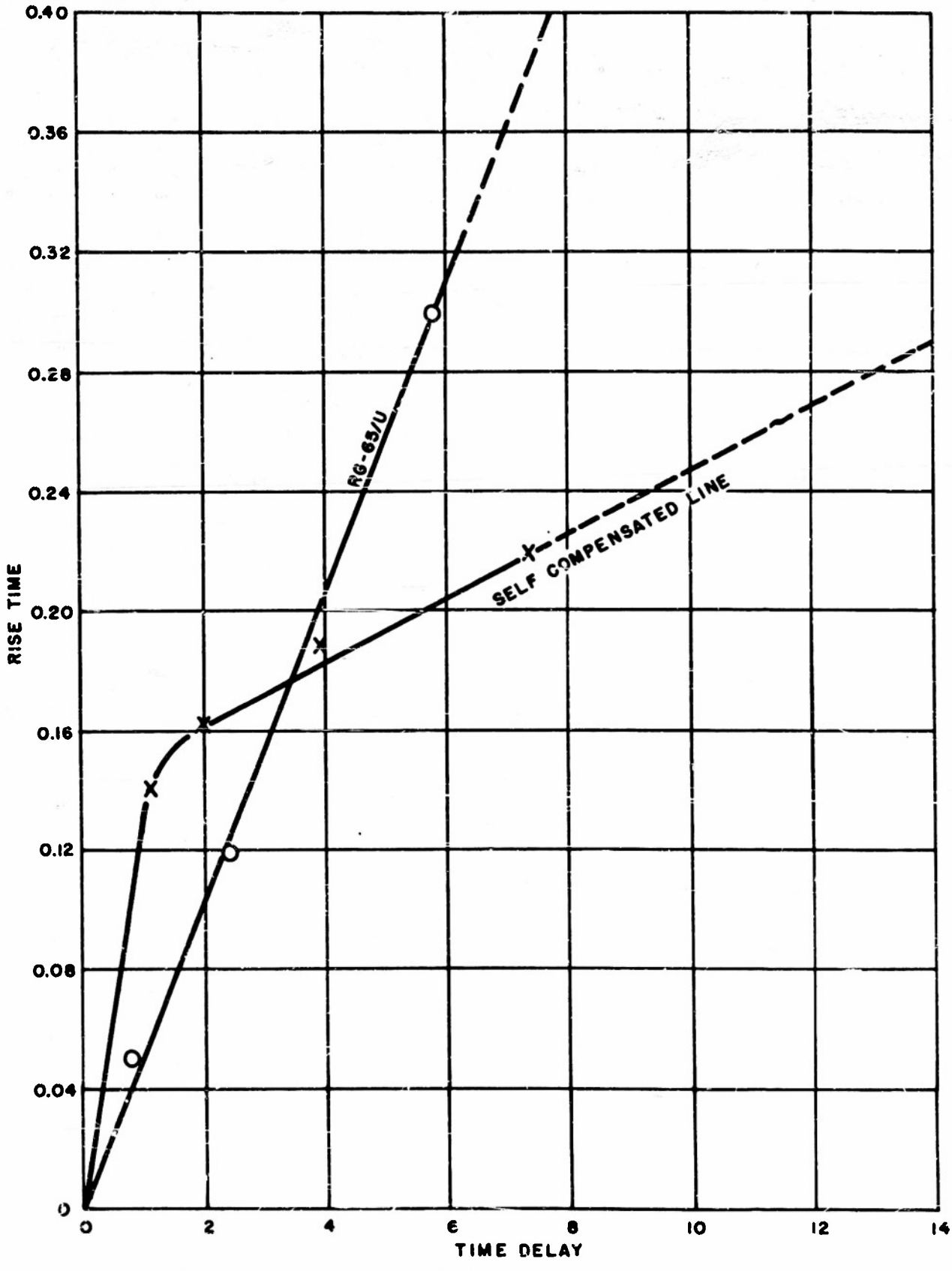

FIG. 24 PLOT OF RISE TIME vs TIME DELAY
FOR SELF COMPENSATED LINES AND RG-65/U DELAY CABLE

NAVORD Report 3759

DISTRIBUTION

	Copies
Chief, Bureau of Ordnance, Navy Department Attn: Re, Re6 Rexg, Re2b, Re4, Re9	 1 2
Commanding General, Wright Air Development Center Wright Patterson Air Force Base Dayton, Ohio Attn: WCERG	2
Director, Naval Research Laboratory Washington 20, D. C. Attn: Technical Information Officer	2
Naval Research Section Library of Congress Washington 25, D. C.	2
Naval Electronics Laboratory San Diego, California	1
Applied Physics Laboratory Johns Hopkins University Silver Spring, Maryland	1
Johns Hopkins University, Radiation Laboratory Baltimore, Maryland	1
Director, Coles Signal Laboratory, SCEL Ft. Monmouth, New Jersey	1
Chief, Engineering and Technical Division Office of the Chief Signal Officer Department of Defense, Washington 25, D. C.	1
Bell Telephone Laboratories Murray Hill, New Jersey	1
Naval Ordnance Test Station (NOTS) Inyokern, California	1
Naval Ordnance Laboratory Corona, California	1
Diamond Ordnance Fuze Laboratory Washington 25, D. C.	1

	Copies
Electrical Engineering Department University of Maryland College Park, Maryland Attn: Mr. George Corcoran	1
Electrical Engineering Department University of Kentucky Lexington, Kentucky Attn: Dr. H. A. Romanowitz	1
Emerson Research Laboratories 701 Lamont Street, N. W. Washington 10, D. C. Attn: W. S. Carley	2